Transportation Research Part C 133 (2021) 103407

Contents lists available at ScienceDirect

Transportation Research Part C

journal homepage: www.elsevier.com/locate/trc

Real-time decentralized traffic signal control for congested urban networks considering queue spillbacks

Mohammad Noaeen [a,c], Reza Mohajerpoor [b], Behrouz H. Far [c], Mohsen Ramezani [d,*]

[a] University of Toronto, Department of Civil and Mineral Engineering, Toronto, Canada
[b] Data61, CSIRO, Sydney, Australia
[c] University of Calgary, Department of Electrical and Software Engineering, Calgary, Canada
[d] The University of Sydney, School of Civil Engineering, Sydney, Australia

ARTICLE INFO

Keywords:
Distributed signal control
Large-scale urban network
Queue spillover
Shockwave model
Traffic operations

ABSTRACT

This paper proposes a decentralized network-level traffic signal control method addressing the effects of queue spillbacks. The method is traffic-responsive, does not require data communication between intersections' controllers, uses lane-based queue measurements, and is acyclic. Each traffic controller operating at an intersection aims at maximizing the effective outflow rate locally and independently with the goal of maximizing global throughput of the entire network. At each intersection, the signal control method estimates and adopts the maximum possible phase time in which all active movements discharge at their full capacity. This is modeled using a shockwave based queue length estimation model while capturing the spillback at the downstream links. The method demands real-time data including, the queue lengths, the arrival flows, and the downstream queue lengths in all the lanes at the control decision times. The proposed method results in a feasible solution in all conditions in the entire network with any scale within a short amount of time. A stability concept for the traffic network is defined, and asymptotic stability of the controlled traffic network are verified. Moreover, a sufficient condition for the optimality of the proposed control algorithm for maximizing the instantaneous total throughput of the network intersections is demonstrated. Numerical results show that the proposed method outperforms benchmark methods in both isolated intersection and network configurations.

1. Introduction

Optimizing and controlling traffic signals is a long-standing concern for most urban cities. Numerous articles have widely attempted to tackle traffic control in different ways, based on various assumptions, goals, and requirements. The existing research works can be broken down from different aspects, including: (i) the scale (isolated Haddad et al., 2010; Yang et al., 2016, arterial Little et al., 1981; Zhang et al., 2015, and network Aboudolas et al., 2010; Mohebifard and Hajbabaie, 2019; Geroliminis et al., 2012; Smith, 2015; Safadi and Haddad, 2021), (ii) the level of responsiveness to traffic (fixed-time or pre-timed Webster, 1958; Allsop, 1971, actuated Zhang and Wang, 2010, and real-time Feng et al., 2015; Christofa et al., 2013; Lee et al., 2017), (iii) the modeling approach (traffic theory based Geroliminis et al., 2012; Michalopoulos et al., 1981; Mohajerpoor and Ramezani, 2019, simulation based Osorio and Selvam, 2017, and data-driven Balaji et al., 2010; Srinivasan et al., 2006), (iv) the type of control method (centralized Diakaki et al., 2003; Dinopoulou et al., 2006; Stevanovic et al., 2015, and decentralized and distributed Lämmer

* Corresponding author.
E-mail address: mohsen.ramezani@sydney.edu.au (M. Ramezani).

https://doi.org/10.1016/j.trc.2021.103407
Received 1 July 2021; Received in revised form 15 September 2021; Accepted 16 September 2021
Available online 20 October 2021

and Helbing, 2008; Le et al., 2015; Chow et al., 2019; Rinaldi and Tampère, 2015; Mehrabipour and Hajbabaie, 2017), (v) the level of congestion condition (undersaturated Mohajerpoor et al., 2019, oversaturated Michalopoulos and Stephanopoulos, 1977; Lo and Chow, 2004, and spillback Geroliminis and Skabardonis, 2011; Ramezani et al., 2017), (vi) the type of estimation method of the input data to the control method (queuing theory Osorio and Bierlaire, 2009, and shockwave model Ramezani and Geroliminis, 2015; Mohajerpoor and Ramezani, 2019), and (vii) the data communication level (traditional Robertson, 1969 and connected vehicle environment Xu et al., 2018; Feng et al., 2015; Emami et al., 2021).

The first step of any traffic-responsive control system is to gather and estimate the input data based on the requirements of the control method. The queue length is an input data that is the base requirement of most traffic signal control methods. Literature suggests two modeling categories to estimate the queue length, (i) the cumulative traffic input–output based models (Webster, 1958; Akçelik, 1999; Erera et al., 1998; Viti and Van Zuylen, 2010), and (ii) shockwave theory-based models (Ramezani and Geroliminis, 2015; Skabardonis and Geroliminis, 2008; Ban et al., 2011; Wu and Liu, 2011). The models in the first category are not inherently able to provide the spatial distribution of queue dynamics (Michalopoulos et al., 1981), suffer from measurement errors, and are not suitable to accurately estimate queue lengths in oversaturated conditions (Vigos et al., 2008). Alternately, the shockwave based models provide the temporal–spatial queue dynamics with input data from loop detectors or probe vehicles. The temporal–spatial feature is essential specifically in oversaturated and spillback conditions. Thus, we develop our control method based on a shockwave based queue length estimation model, which needs arrival flow and initial queue length data in real-time and is reasonably accurate as it captures queue length evolution in time and space. It is worth noting that the queue spillback phenomenon can be captured by the Cell Transmission Model (CTM) (Daganzo, 1995), Link Transmission Model (LTM) (Yperman et al., 2005), learning-based approaches (Lee et al., 2019), and shockwave models. However, the shockwave model requires less information compared to the three other models (Nie and Zhang, 2005).

In addition to the level of accuracy, the number of required data types, and the capabilities of capturing the details of traffic behaviors, there are other factors that impact the effectiveness of the traffic signal control method. These factors include the volume of the data, the cost-effectiveness of data collection in the real world, the time and the degree of simplicity of the data processing for estimation and signal timing, and the amount of data communication. The type of traffic control method identifies the amount of impact of these factors, specifically on the challenges of data gathering, processing, and transmission. With regards to the type of traffic control methods, centralized systems provide a unified control entity that acts centrally, based on the collected data from the sensors and the measurements and computation over the entire network. These approaches do not scale well when they are applied to control large urban networks. As a solution to the scaling problem, distributed and decentralized systems present more than one decision-making unit where they do not contain any centralized controller that coordinates or generates traffic plans. Although there is not a general agreement on the usage of distributed and decentralized in the literature of network traffic signal control and the two terms are used interchangeably, we use them as follows.

In distributed systems, every single intersection controller is an independent agent that makes its own decisions in interactions with other neighbor intersections. In these systems, there is information exchange between neighbor intersections and the decisions might be made by negotiation between the intersections. In contrast, decentralized systems require local data only. In decentralized systems, the local controllers have no interactions with other intersections in terms of both input and output data in decision-making computations. This way, the reliability of the system increases by removing the need for communications between intersections. Thus, communication issues, such as network delays, do not affect the control system. Decentralized systems in the literature of network traffic signal control may sometimes be referred to as fully distributed system. For instance, Gershenson (2007) proposed a local self-regulation approach in which a phase receives green time if the number of vehicles on an approach meets a predefined threshold. In another work, Burguillo-Rial et al. (2012) proposed a self-organizing control method relying on stop-bar detectors. Furthermore, Lämmer and Helbing (2008) proposed a self-control method that equalizes the degree of saturation and queue length. Another approach was proposed by Xie et al. (2012), that modeled the single intersection control problem as a single machine-scheduling problem. The approach operates based on aggregating arriving vehicles in clusters, where clusters are defined as jobs in the scheduling problem.

The pressure-driven traffic control policies P_0 and Max Pressure (MP) are noteworthy research works in the area of distributed and decentralized traffic control. Smith (1980) introduced the P_0 control method, which considers variable route choices and maximizes network capacity under certain conditions, where demand is within network capacity, and there is no spillback. This method was revisited by Smith (2011) and Smith et al. (2019). MP was originally presented by Tassiulas and Ephremides (1990) in a wireless packet switching network. Varaiya (2013) applied and developed MP for an urban traffic network. This local feedback controller controls traffic signals based on the difference in traffic load on the upstream and downstream links of the intersection. Varaiya (2013) formally proved that MP can stabilize a traffic network when the network inflows are within the network capacity and there is no spillback. Since then, many research works attempted to adapt the method to real-world applications. For instance, Gregoire et al. (2014), proposed a method to consider finite link capacity, i.e., bounded queue, while the assumption in the preliminary method relies on infinite road capacities. The MP method is also employed to stabilize the queues in signalized arterial network (Kouvelas et al., 2014). The preliminary method (i.e., Varaiya, 2013) performs an acyclic control, where cycle length and composition can vary during the process. An extension is a cyclic MP-based algorithm proposed by Le et al. (2015) to provide a minimum phase in a cycle for the movements with low traffic demand. Further, Li and Jabari (2019) proposed a decentralized MP-based method, called position-weighted backpressure (PWBP) that captures the spatial distribution of vehicles along the links, and consequently, spillback conditions. The results showed that PWBP method outperforms the standard and the capacity-aware MP methods, specifically with higher demand levels.

It should be pointed out that the PWBP method proposed by Li and Jabari (2019) employs a capacity-aware version of MP which additionally accounts for the possibility of spillbacks by considering spatial distribution of vehicles through applying higher weights to queues that extend to the ingress of the link. In the method, a small number of phases (i.e. 4 – 8 possible phases) are used. In our proposed method, the phase with the highest estimated effective outflow rate receives the priority. The notable difference is that our proposed method also optimizes the phase duration while the underlying traffic model is different. Our method is explicitly based on shockwave theory. Moreover, in our proposed method, all possible phases (with any number of non-conflicting movements) are explored to determine the optimal phase.

Having considered the requirements discussed above, we propose a DEcentralized Spillback Resistant Acyclic (DESRA) signal control algorithm for a large scale network. Our proposed control method is fully decentralized, which makes it independent of data communication among intersections in the network. This independence is essential from two aspects. First, during the estimation step, the method removes the need for exchanging input (estimated) data between intersections. Second, each intersection does not need to share its control decisions with other intersections. These two factors contribute to decreasing the processing time of the method. Another feature of the proposed method is that it is acyclic, which removes the need to determine cycle times and pre-determined sequence of phases in a cycle. This increases the frequency of decision points during the signal timing process and helps provide higher flexibility in traffic-responsive solutions.

The proposed control method is a discrete-time optimization that explores the maximum possible phase time in which all active movements discharge at their full capacity. This is fulfilled based on finding the minimum saturated green time (greater than zero) for all possible phases. The proposed method averts from dealing with minimizing or maximizing any variables. In turn, the control method simply finds the minimum and maximum of estimated parameters, such as saturated green time and effective outflow rate in each lane. Therefore, it is not trapped in the optimization process' challenges and complexities. This feature of the method leads to have a feasible solution in all traffic conditions. Moreover, it ensures a calculation time of less than a second, which empowers the method for real-time applications.

In the network scale, avoiding or reducing the queue spillback phenomena is crucial, as it significantly reduces the outflow of the network. Therefore, to avoid the spillback condition in the proposed method, we consider the real-time available storage capacity of the downstream link as a constraint to limit the optimal green time of each upstream movement. The available storage capacity of the downstream link is calculated based on the queue length in the downstream link, which is read at the time of decision-making. Moreover, a new stability concept for the network-wide traffic is defined, and the robust and asymptotic stability of the controlled traffic network are comprehended. It is also shown that the proposed traffic control method pertains optimal characteristics under certain conditions.

The rest of this paper is organized as follows. Section 2 describes the problem statement. Section 3 presents the proposed decentralized traffic control method. Section 4 discusses the stability and optimality of the traffic network. Simulation setup and results are discussed in Section 5. Finally, Section 6 summarizes the paper and sketches potential directions for further research.

2. Problem statement

Let us consider an urban network with multiple intersections indexed by $i \in \{1, \dots, I\}$ (I is the total number of intersections), wherein each intersection is controlled independently in a fully decentralized system without any coordination methods. Let each intersection be a general 4-way signalized intersection with lanes in which only one movement is served, whether left-turn, through, or right-turn movement. The traffic movements $j \in \mathcal{J}_i = \{1, 2, \dots, J_i\}$ can be activated at intersection i, i.e. receive green signal indications, or deactivated, i.e. receive red signal indications. A phase at intersection i is defined as a set of non-conflicting movements that indicates whether the movements at the intersection are activated or deactivated during the time called phase time p_i. During the phase time, one or several non-conflicting movements are activated and simultaneously receive the right of way and all other movements are deactivated. All possible phases at intersection i are collected in set $\boldsymbol{\Phi}_i$. $\mathcal{P}_i$ is a possible phase in the set $\boldsymbol{\Phi}_i$. We assume the discrete-time event index at intersection i is k_i, $k_i \in \{0, 1, \dots\}$. Moreover, $\lambda_{ji}(k_i) \in \{0, 1\}$, where 0 and 1 respectively represent red and green signal indications at k_i; $(\lambda_{ji}(k_i))$ denotes a $i \times j$ matrix with λ_{ji} elements.

The control decisions of each intersection are made independently of other intersections at each decision point k_i. The time instant in which the control decisions are made is called the phase transition point $t(k_i)$, and $t(k_i + 1) - t(k_i) = p_i(k_i) + \mathcal{I}_i(k_i)$, where $p_i(k_i)$ is the phase duration at the intersection at k_i and $\mathcal{I}_i$ is the interphase. (Note that the interphase can be green, yellow, or red signal for different movements, see Fig. 5 for more information). At each phase transition point, the following real-time input data in all the lanes at the intersection are collected: (i) the queue lengths, (ii) the arrival flows, and (iii) the downstream queue lengths. The control decisions include the optimal phase time $p_i^*(k_i)$, the optimal phase $\mathcal{P}_i^*(k_i)$, and the interphase $\mathcal{I}_i^*(k_i)$. The three control decisions are integrated and represent the ideal phase, $\psi_i^*(k_i) = (p_i^*(k_i), \mathcal{P}_i^*(k_i), \mathcal{I}_i{}^*(k_i))$. The objective is to find an ideal phase $\psi_i^*(k_i)$ at each decision point to maximize the number of vehicles that exit the approaches at the intersection, i.e. the intersection throughput. The premise is that the ideal phase would enable movements to discharge at their maximum capacity. Accordingly, it can be conjectured that no other phase can lead to higher intersection throughput.

3. Decentralized spillback resistant acyclic (DESRA) traffic signal control algorithm

In this section, the details of the proposed DESRA traffic signal control scheme for a generic network are presented. The flowchart in Fig. 1 helps clarify the process of the proposed method, which is applied to each intersection independently. The proposed method is explained according to the control decisions, (i) phase time calculation and (ii) phase improvement and interphase determination. Prior to that, we provide the details of estimating saturated green time without considering spillback effect (Section 3.1) and in general case considering the effect of spillback (Section 3.2).

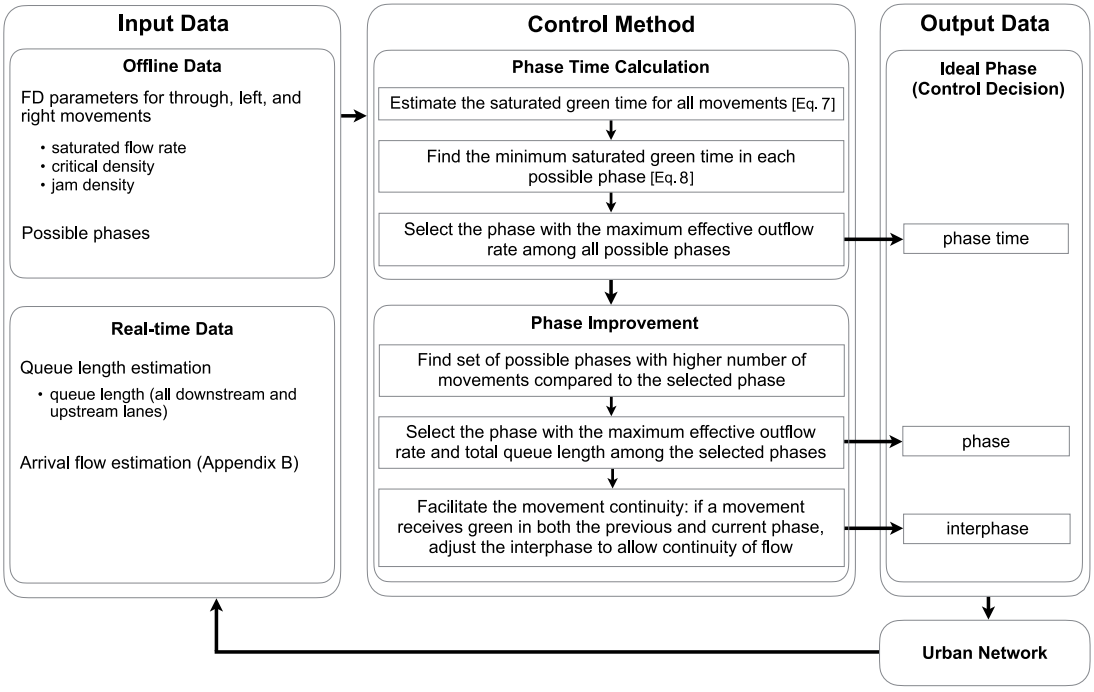

Fig. 1. Flowchart of the proposed traffic signal control method.

3.1. Saturated green time: without spillback control

The saturated green time, $G_{ji}^{\mathrm{sat}}(k_i)$, which is estimated for each movement at the decision point k_i is defined as the maximum green time that movement j at intersection i can discharge vehicles at its full capacity (i.e. the saturation flow). Theoretically, saturated green time guarantees the maximum effective outflow rate of the vehicles, assuming the arrival rate to the back of the queue is smaller than the saturation flow.

The nominal saturated green time, shown by $G_{ji}^{\mathrm{s}}(k_i)$, is the saturated green time assuming that there is sufficient storage capacity at the downstream link of movement j, and is calculated based on the LWR (Lighthill–Whitham–Richards) theory (Lighthill and Whitham, 1955; Richards, 1956) as follows:

$$G_{ji}^{\mathrm{s}}(k_i) = \frac{x_{ji}^{0}(k_i)(\mathcal{K}_{ji}^{\mathrm{jam}} - \mathcal{K}_{ji}^{\mathrm{arr}}(k_i))}{S_{ji} - q_{ji}^{\mathrm{arr}}(k_i)}, \tag{1}$$

where $\mathcal{K}_{ji}^{\mathrm{jam}}$ and S_{ji} are the jam density and the saturation flow of movement j at intersection i, respectively. Moreover, $x_{ji}^{0}(k_i)$, $\mathcal{K}_{ji}^{\mathrm{arr}}(k_i)$, and $q_{ji}^{\mathrm{arr}}(k_i)$ respectively denote the queue length, and estimated arrival density and flow of movement j at the intersection at the time instant $t(k_i)$.

To estimate the saturated green time, three parameters and two variable inputs are required. The parameters include (1) saturation flow S_{ji}, (2) critical density $\mathcal{K}_{ji}^{\mathrm{cri}}$, and (3) jam density $\mathcal{K}_{ji}^{\mathrm{jam}}$. The parameters can be readily estimated from the flow-density Fundamental Diagrams (FDs) that are constructed individually for all three turns (i.e. left, through, and right turns) in an offline process. A common assumption in the literature is to assume triangular flow-density FDs. Consequently, $\mathcal{K}_{ji}^{\mathrm{arr}}(k_i)$ is:

$$\mathcal{K}_{ji}^{\mathrm{arr}}(k_i) = \frac{q_{ji}^{\mathrm{arr}}(k_i)\mathcal{K}_{ji}^{\mathrm{cri}}}{S_{ji}}. \tag{2}$$

With a limited link length for movement j at intersection i, Δ_{ji}, the propagation of shockwaves in queue buildup evolution is constrained. This constraint is enforced by spillback conditions and may adversely affect the saturated green time $G_{ji}^{\mathrm{sat}}(k_i)$. Hence, let us define the estimated maximum queue extent, $x_{ji}^{\mathrm{M}}(k_i)$, as:

$$x_{ji}^{\mathrm{M}}(k_i) = \frac{x_{ji}^{0}(k_i)(\mathcal{K}_{ji}^{\mathrm{jam}} S_{ji} - q_{ji}^{\mathrm{arr}}(k_i)\mathcal{K}_{ji}^{\mathrm{cri}})}{\mathcal{K}_{ji}^{\mathrm{jam}}(S_{ji} - q_{ji}^{\mathrm{arr}}(k_i))}. \tag{3}$$

As shown in Fig. 2, when the estimated maximum queue extent, $x_{ji}^{\mathrm{M}}(k_i)$, exceeds the link length, the two backward-moving shockwaves, $SWI_{ji}(k_i)$ and $SWR_{ji}(k_i)$, cannot theoretically intersect each other because of the link length limitation. To accommodate

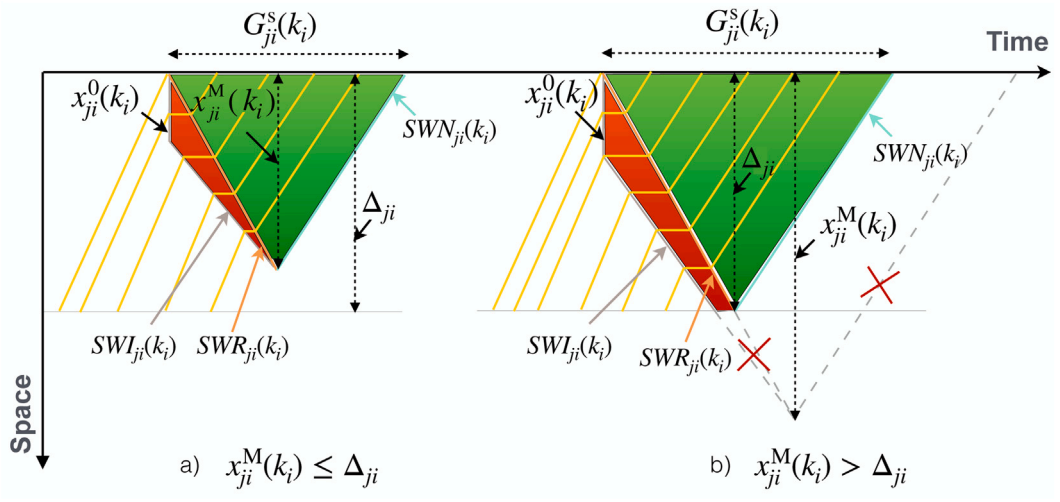

Fig. 2. Shockwave analysis of the saturated green time estimation: (a) estimated maximum queue extent is less than or equal to the link length and (b) estimated maximum queue extent is greater than the link length.

this condition, $G^{s}_{ji}(k_i)$ based on the triangular FD is:

$$G^{s}_{ji}(k_i) = \begin{cases} \frac{x^{M}_{ji}(k_i)\kappa^{jam}_{ji}}{s_{ji}} & x^{M}_{ji}(k_i) \le \Delta_{ji} \\ \frac{\Delta_{ji}\kappa^{jam}_{ji}}{s_{ji}} & x^{M}_{ji}(k_i) > \Delta_{ji}. \end{cases} \tag{4}$$

Note that, $G^{s}_{ji}(k_i)$ in the first condition of Eq. (4) is equivalent to Eq. (1). We should also point out that the critical and jam points on the pre-determined FD are fixed and accordingly $SWR_{ji}(k_i)$ has a fixed slope. The slope of $SWI_{ji}(k_i)$ depends on FD and real-time arrival flow. Therefore, there is no guarantee that the shockwaves $SWI_{ji}(k_i)$ and $SWR_{ji}(k_i)$ intersect each other at the far end of the link. Nonetheless, if they do not intersect, the calculation of saturated green time depends only on $SWR_{ji}(k_i)$ and $SWN_{ji}(k_i)$ shockwaves, not on $SWI_{ji}(k_i)$ shockwave.

Besides the three FD parameters, queue length $x^{0}_{ji}(.)$ and arrival flow $q^{arr}_{ji}(.)$ are two variable inputs required to make the control decision. They are assumed to be either available, e.g. via traffic cameras, loop detectors, or estimated based on historical and/or real-time data. In the microsimulation tests, the required data (the vehicle counts) to measure the arrival flow is collected through detectors at the far end upstream of each approach of the intersection. For arrival flow measurement, a discretization method is used that is presented in Appendix B. To estimate queue length in each lane, we use the available data during the simulation at each decision point. There are no requirements on the choice of queue length measurement devices and estimation methods. It should be noted that although the proposed method is decentralized and the traffic signal controller in each intersection only uses the data of its incoming and outgoing links, the queue length data of incoming and outgoing links of each intersection is shared with four immediate adjacent intersections. In other words, the queue length data of a link simultaneously affect the decision making of the two intersections at up and downstreams.

3.2. Saturated green time: considering spillback control

At isolated intersections, it is assumed that there are no storage capacity restrictions in downstream links. However, in the network, storage capacities of links are limited and the discharge time of the upstream approach is restricted based on the available storage capacity of the downstream link. Hence, in spillback control, the impact of the downstream queues on the signal timing control decisions is considered.

Let us assume that $x^{d}_{ji}(k_i)$ is the available storage capacity of the link downstream of movement j of intersection i at decision point k_i, $G^{d}_{ji}(k_i)$ is the maximum time that the link downstream of movement j can let vehicles in at the decision point k_i, and Δ^{d}_{ji} is the downstream link length. Note that we define $x^{d}_{ji}(k_i)$ for the downstream link, not the downstream lanes. This definition is chosen as a conservative measure because discharged vehicles from the upstream link might use any of the downstream lanes. In addition, discharge interruptions might happen when the vehicles get stuck in the downstream lanes while trying to change lanes. Therefore, we consider that the available storage capacity of a downstream lane depends on the available storage capacity of the downstream link, which is the minimum available storage capacity in all the lanes in the link. For this purpose, let $x^{0d}_{ji}(k_i)$ be the

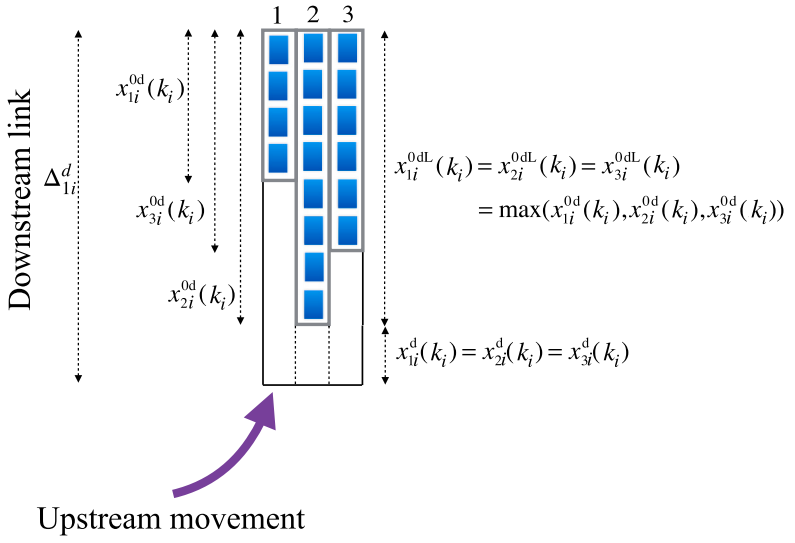

Fig. 3. Considering the available storage capacity of the downstream link as the available storage capacity of all the downstream lanes.

queue length of the movement j in the downstream link. We also define $x_{ji}^{0dL}(k_i)$ to represent the maximum queue length among all the lanes in the downstream link. Consequently,

$$x_{ji}^{d}(k_i) = \Delta_{ji}^{d} - x_{ji}^{0dL}(k_i). \tag{5}$$

As illustrated in Fig. 3, the available storage capacity of all the downstream lanes is considered to be the same and equal to the available storage capacity of the link. Note that if more details of real-time information on lane-choice of vehicles is available, this can be readily incorporated in the proposed method. The current assumption is a simple solution to lane choice as this is difficult to be obtained in practice in real-time.

The spillback constraint states that if the estimated saturated green time of upstream movement j, $G_{ji}^{sat}(k_i)$, is greater than the available time capacity of the link downstream of movement j, $G_{ji}^{d}(k_i)$, $G_{ji}^{sat}(k_i)$ is limited to $G_{ji}^{d}(k_i)$ (see Fig. 4), i.e. $G_{ji}^{sat}(k_i) = \min\{G_{ji}^{s}(k_i), G_{ji}^{d}(k_i)\}$, where:

$$G_{ji}^{d}(k_i) = \frac{x_{ji}^{d}(k_i)\mathcal{K}_{ji}^{jam}}{S_{ji}}. \tag{6}$$

Remark 1. Note that $x_{ji}^{d}(k_i)$ is the maximum queue length that downstream link can accommodate the vehicles traveling from the upstream lane. When the entire queue of the upstream lane cannot be discharged due to the downstream capacity restriction, in Eq. (6), $x_{ji}^{d}(k_i)$ is considered equivalent to the maximum possible queue extent that can be discharged from the upstream lane. S_{ji} and $\mathcal{K}_{ji}^{jam}$ are then related to the upstream lane.

$G_{ji}^{d}(k_i)$ is estimated based on two assumptions, (i) capacity flow from the upstream link and (ii) zero outflow for the downstream link. Note that the queue length variations of the downstream lanes or links are not considered in estimating the available storage capacity of the downstream movements, and only the queue length evolution of the upstream lane is taken into account. The reason is that during the selected phase time, the only source of queue length growth is the upstream queue. As stated earlier, the destination of all movements in either of the possible phases are distinct; thus, during a phase, there is no inflow to a downstream link except from only one movement in one of the upstream links. Considering the queue discharge dynamics of the downstream lanes within a phase time may result in determining a longer phase, as the links may provide greater storage capacities over time. However, we ignore this useful information, since it requires extra data from all the immediate downstream traffic signals, i.e. traffic signal states and timings. Nevertheless, two considerations in the proposed acyclic method mitigate the downside of ignoring this information; (i) movement continuities (see Section 3.4) and (ii) shorter time interval between the decision points. Therefore, the estimation method is conservative and yet effective to estimate $G_{ji}^{d}(k_i)$. Being conservative is consistent with the previous assumption on estimation of $x_{ji}^{d}(k_i)$. Note that although the proposed method is presented with one lane per movement, it can be easily extended to multiple lanes per movement.

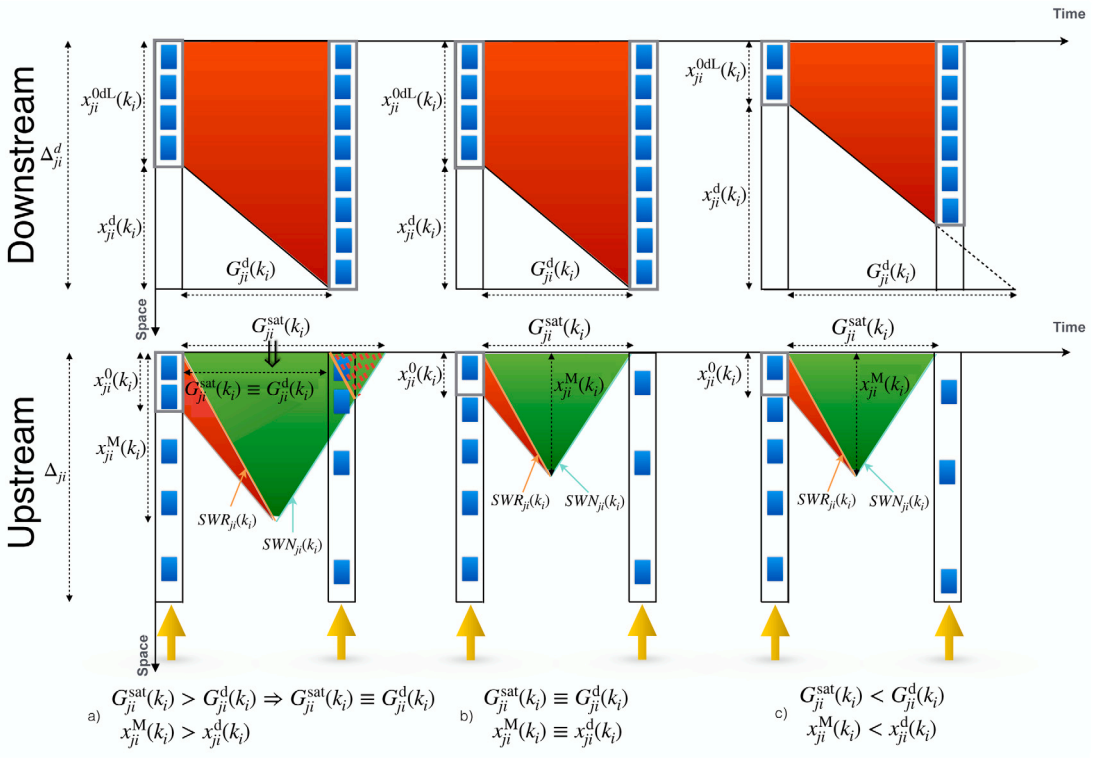

Fig. 4. Shockwave analysis of the saturated green time estimation when the storage capacity of the downstream link is limited: (a) the upstream estimated maximum queue extent is greater than the available storage capacity of the downstream movement, (b) the upstream estimated maximum queue extent is equal to the available storage capacity of the downstream movement, and (c) the upstream estimated maximum queue extent is less than the available storage capacity of the downstream movement.

Eventually, we can combine the conditions in estimating the saturated green time $G_{ji}^{\text{sat}}(k_i)$ in non-spillback and spillback conditions as below:

$$G_{ji}^{\text{sat}}(k_i) = \begin{cases} \frac{x_{ji}^{\text{M}}(k_i)\kappa_{ji}^{\text{jam}}}{S_{ji}} & x_{ji}^{\text{M}}(k_i) \le x_{ji}^{\text{d}}(k_i) \;\&\; x_{ji}^{\text{M}}(k_i) \le \Delta_{ji} \\ \frac{\Delta_{ji}\kappa_{ji}^{\text{jam}}}{S_{ji}} & \Delta_{ji} \le x_{ji}^{\text{M}}(k_i) \;\&\; \Delta_{ji} \le x_{ji}^{\text{d}}(k_i) \\ \frac{x_{ji}^{\text{d}}(k_i)\kappa_{ji}^{\text{jam}}}{S_{ji}} & x_{ji}^{\text{d}}(k_i) \le x_{ji}^{\text{M}}(k_i) \;\&\; x_{ji}^{\text{d}}(k_i) \le \Delta_{ji} \end{cases} \tag{7}$$

3.3. Phase time calculation

Here, based on the estimated saturated green time in Section 3.2, the minimum saturated green time greater than zero for each possible phase at the decision point k_i, $G_i^{\min}(\mathcal{P}_i, k_i)$, is:

$$G_i^{\min}(\mathcal{P}_i, k_i) = \min_{j \in \mathcal{M}_{\mathcal{P}_i}} G_{ji}^{\text{sat}}(k_i) \qquad G_{ji}^{\text{sat}}(k_i) > 0, \tag{8}$$

where $\mathcal{M}_{\mathcal{P}_i}$ is the set of movements in phase $\mathcal{P}_i$ that receive the right-of-way.

After finding $G_i^{\min}(\mathcal{P}_i, k_i)$, the next step is calculating the maximum of the estimated effective outflow rate of vehicles in each possible phase. To this end, first the vehicle discharge of each movement in each possible phase based on the shockwave model given the green time $G_i(\mathcal{P}_i, k_i)$ is obtained as:

$$F_{ji}(\mathcal{P}_i, k_i) = \begin{cases} S_{ji} G_i(\mathcal{P}_i, k_i)\lambda_{ji}(k_i) & G_{ji}^{\text{sat}}(k_i) \ge G_i(\mathcal{P}_i, k_i) \\ \left(S_{ji} G_{ji}^{\text{sat}}(k_i) + q_{ji}^{\text{arr}}(k_i)(G_i(\mathcal{P}_i, k_i) - G_{ji}^{\text{sat}}(k_i))\right)\lambda_{ji}(k_i) & G_{ji}^{\text{sat}}(k_i) < G_i(\mathcal{P}_i, k_i) \;\&\; x_{ji}^{\text{M}}(k_i) \le x_{ji}^{\text{d}}(k_i) \\ S_{ji} G_{ji}^{\text{sat}}(k_i)\lambda_{ji}(k_i) & G_{ji}^{\text{sat}}(k_i) < G_i(\mathcal{P}_i, k_i) \;\&\; x_{ji}^{\text{M}}(k_i) > x_{ji}^{\text{d}}(k_i). \end{cases} \tag{9}$$

For each possible phase the total estimated effective outflow rate during the determined phase time of the possible phase (including the phase's total lost time), $v_i(\mathcal{P}_i, k_i)$, is calculated as:

$$v_i(\mathcal{P}_i, k_i) = \frac{\sum_{j \in \mathcal{M}_{\mathcal{P}_i}} F_{ji}(\mathcal{P}_i, k_i)}{G_i(\mathcal{P}_i, k_i) + L_i(k_i)}, \tag{10}$$

where L_i is the phase lost time including start-up and clearance lost times. Let us define $F_{ji}^{\max}(\mathcal{P}_i, k_i) = S_{ji} G_i^{\min}(\mathcal{P}_i, k_i) \lambda_{ji}(k_i)$. The optimum phase $\mathcal{P}_i^*(k_i)$ at decision point k_i is selected to maximize the effective outflow rate $v_i(\mathcal{P}_i, k_i)$:

$$\mathcal{P}_i^*(k_i) = \text{Argmax}_{\mathcal{P}_i} \left\{ v_i^{\max}(\mathcal{P}_i, k_i) \right\}, \tag{11}$$

where $v_i^{\max} = \sum_{j \in \mathcal{M}_{\mathcal{P}_i}} F_{ji}^{\max}(\mathcal{P}_i, k_i) / (G_i^{\min}(\mathcal{P}_i, k_i) + L_i(k_i))$.

Since more than one possible phase might be found with the maximum effective outflow rate, we select one phase in this step (i.e. iteration 1), and call it $\mathcal{P}_{i,\text{Iter1}}^*(k_i)$. The selected phase in this iteration might change in accordance with the process of phase improvement introduced in Section 3.4, which adds to the movements of the selected phase for maximizing the outflow of the vehicles and decreasing the effect of the long queues.[1] Hence, the ideal phase time $p_i^*(k_i)$ in the first iteration can be calculated as below:

$$p_i^*(k_i) = G_i^{\min}(\mathcal{P}_{i,\text{Iter1}}^*, k_i). \tag{12}$$

Note that in the first iteration, only the first condition of Eq. (9) is used to calculate the effective outflow of each active movement because the estimated saturated green times of all movements in each phase are greater than or equal to the selected minimum saturated green time for the phase. The throughput of the network can be further increased after applying the heuristic proposed in Section 3.4.

3.4. Phase improvement

A phase can, at most, include a certain number of active movements, called maximum movements. Suppose that the selected phase in Section 3.3 contains a lower number of movements than the maximum movements. Allowing other non-conflicting movements to be activated can provide an opportunity to increase the intersection outflow during the selected phase time $p^*(k_i)$. By this consideration, movements with under-saturated conditions might also appear in the phase and here the second condition of Eq. (9) is used in the calculation of the outflow of the extra undersaturated movements in a phase. Consequently, we do a second iteration to explore the ideal phase with a higher number of movements (if available) based on the finalized phase time, $p^*(k_i)$. To this end, first we find the possible phases that encapsulate the active movements of the selected phase in the first iteration. Here, we end up with a new set of possible phases, $\mathcal{P}_i^{\text{Iter2}}(k_i)$, such that $\mathcal{P}_i^{\text{Iter2}}(k_i) \subseteq \boldsymbol{\Phi}_i$. Then, we apply the same process provided in Section 3.3 over the new set of phases determined in this step (i.e. $\mathcal{P}_i^{\text{Iter2}}(k_i)$) to find a phase or a set of phases with a higher effective outflow rate, i.e. $\mathcal{P}_{i,\text{Set}-\text{Iter2}}^*(k_i)$. We should note that the additional movements added to the selected phase in Section 3.3, $\mathcal{P}_{i,\text{Iter1}}^*(k_i)$, can contain queues which exceed the available storage capacity of their related downstream lane. As vehicles do not enter the intersection when facing a spillover in the downstream lane, we do not remove the phases that include these movements from the possible phases of $\mathcal{P}_i^{\text{Iter2}}(k_i)$.

Following the process in increasing the number of activated movements in the selected phase, the method may find more than one possible phase in the set $\mathcal{P}_{i,\text{Set}-\text{Iter2}}^*(k_i)$. To help with reducing the long queues issue, which can negatively impact the performance of the signal timing method, the method selects a phase among the phases in the set $\mathcal{P}_{i,\text{Set}-\text{Iter2}}^*(k_i)$ that contains a larger total queue length. This is done by finding the total queue length of each possible phase in the set of possible phases, $\mathcal{P}_{i,\text{Set}-\text{Iter2}}^*(k_i)$. Next, the phase with maximum total queue length is selected as the ideal phase, $\mathcal{P}_{i,\text{Iter2}}^*(k_i)$. However, before the phase is activated, sub-phase called interphase, $\mathcal{I}_i(k_i)$, is required to be activated. The interphase time is equal to yellow time (e.g. 3 s). The possible signal indications in an interphase are red, green, or yellow. Fig. 5 provides a visual illustration of the four possible cases.

The interphase is determined based on the selected phase and previous phase. States **a**, **b**, and **c** might regularly happen in a cyclic signal control. However, in the proposed acyclic method, when the selected phase and previous phase are both green, a green interphase lets the vehicles in a movement remain discharging without any interruption and maintains the movement continuity between the two successive phases. This reduces the number of unnecessary yellow times, hence, vehicles' stops (see Fig. 5**d**). If the selected and previous phases are, respectively, red and green, the traffic light is considered to stay red during the interphase to manage the movements' conflicts, see Fig. 5**c**. We should point out that the decision point k_i is determined through the calculation of the phase time in the previous decision point, i.e. $k_i - 1$. The sum of the phase and interphase times at the decision point $k_i - 1$ specifies the next decision point, i.e. k_i. It is apparent that decision points for each intersection are unique.

4. Stability and optimality of the proposed traffic signal control method

In this section, we discuss the stability and also optimality of the traffic network as a result of implementing the proposed decentralized traffic control paradigm. To this aim, a new stability condition is defined for the traffic network in the time duration $[0, T]$. The duration can cover any desired time period of interest, e.g. the morning or afternoon peak periods.

[1] In this step, there may be two or more phases with the same or different number of movements that provide the same effective outflow as a maximum effective outflow. To reduce the unnecessary computation efforts, we ignore finding several phases to improve. Instead, we select the phase associated with the first occurrence of maximum effective outflow, and improve it later in further steps.

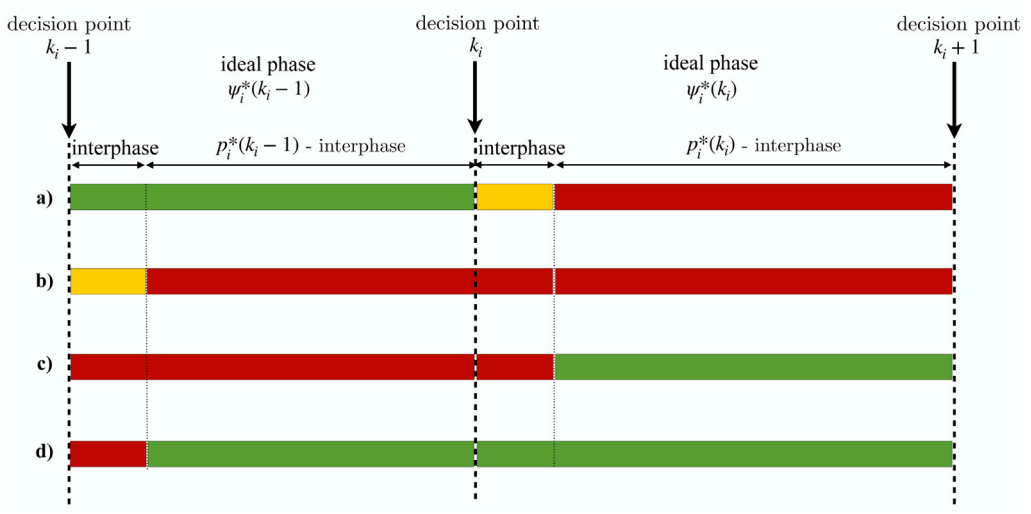

Fig. 5. Interphase at time step k_i based on phase decisions at time steps $k_i - 1$ and k_i **(a)** if phase $k_i - 1$ is green and phase k_i is red, the interphase is yellow, **(b)** if phase $k_i - 1$ is red and phase k_i is red, the interphase is red, **(c)** if phase $k_i - 1$ is red and phase k_i is green, the interphase is red, and **(d)** if phase $k_i - 1$ is green and phase k_i is green, the interphase is green. (For interpretation of the references to color in this figure legend, the reader is referred to the web version of this article.)

4.1. Stability of the traffic network

Definition 1. The traffic network is called α-stable in the duration $[0, T]$ ($\alpha \leq 1$ is a positive constant), if given the event sequence $\{k_i\} = \{k_i | t(k_i) \in [0, T]\}$ and control sequence $\{(\lambda_{ji}(k_i), p_i(k_i))\}$ at every intersection and for every movement we have

$$1/n_i \sum_{k_i} \left(q_{ji}^{\text{arr}}(k_i) p_i(k_i) - F_{ji}(\mathcal{P}_i, k_i) \right) \leq \alpha \Delta_{ji} K_{ji}^{\text{jam}} \qquad \forall i \in \{1, \dots, I\}, j \in \mathcal{J}_i, \tag{13}$$

where $n_i = |\{k_i\}|$.

Definition 1 implies that the average number of vehicles on every link of the network during the period $[0, T]$ (i.e. the average queue length at the link) should be less than α proportion of the link's storage capacity $\Delta_{ji} K_{ji}^{\text{jam}}$. Note that in inequality (13) the links are assumed to possess infinite capacity, and the queue lengths at the intersection are not limited to the link length Δ_{ji}. It is clear that α should be a positive value, since the number of vehicles exiting a link cannot be larger than the number of vehicles entering it, and the queue size at the link is greater than zero at least during the red phases facing the movements served by the link. Let us assume that $\mathcal{J}_{\text{E}}$ is the set of entrance links to the network. Based on the above definition, an admissible demand (arrival flows of the entering links to the network) can be defined as follows.

Definition 2. A demand sequence $\{q_l^{\text{E}}(t)\}$ ($l \in \mathcal{J}_{\text{E}}$) is admissible in time interval $[0, T]$, if there exists a control sequence $\{(\lambda_{ji}(k_i), p_i(k_i))\}$ ($\{k_i\} = \{k_i | t(k_i) \in [0, T]\}$) for every movement $j \in \mathcal{J}_i$ at each intersection i, such that the traffic network is α-stable.

Theorem 1. *The DESRA control strategy results in an α-stable signalized traffic network for some $\alpha \leq 1$, if and only if the network's demand is admissible in the sense of Definition 2.*

Proof. It is clear that if the demand is not feasible according to Definition 2, there is no control sequence $\{(\lambda_{ji}(k_i), p_i(k_i))\}$ that results in an α-stable traffic network. We now prove the sufficiency part of the theorem assuming that the demand is feasible, just considering the optimal phase $\mathcal{P}_i^*(k_i) = \mathcal{P}_{i,\text{Iter}1}^*(k_i)$ for the sake of this proof. It is clear that additional movements that are appended in the phase improvement step (see Section 3.4), further strengthens the stability of the network.

First consider the internal network links, i.e. $\mathcal{J}_{\text{in}} = \{\{\mathcal{J}_i\} - \mathcal{J}_{\text{E}}\}$ ($i \in \{1, \dots, I\}$). According to Eq. (7), the DESRA algorithm does not give a green time permit to any upstream link of link $j \in \mathcal{J}_{\text{in}}$ if there is no sufficient storage capacity at the link. Hence, the algorithm intrinsically enforces $1/n_i \sum_{k_i} q_{ji}^{\text{arr}}(k_i) p_i(k_i) \leq \Delta_{ji} K_{ji}^{\text{jam}}$ for all $j \in \mathcal{J}_{\text{in}}$. This concludes that condition (13) is fulfilled for $\alpha = 1$.

Moreover, the DESRA algorithm maximizes the effective outflow rate $v_i(\mathcal{P}_i, k_i)$ at each time-step k_i, where $\mathcal{P}_i = \mathcal{P}_i^*(k_i)$. Therefore, the total effective outflow at the intersection and the effective outflow of every critical movement of the activated phase (i.e. $j \in \mathcal{M}_{\mathcal{P}_{i,\text{Iter}1}^*}$) are maximized at each time-step taking the storage capacity of the downstream links into account. In other words, the expression $1/n_i \sum_{k_i} F_{ji}(\mathcal{P}_i, k_i)$ is maximized due to the DESRA scheme for every movement at every intersection in the

network. Accordingly, given demand sequence $\{q_j^{\mathrm{E}}(t)\}$ if inequality (13) is not satisfied for some $j \in \mathcal{J}_{\mathrm{E}}$ by applying the control sequence $\{(\lambda_{ji}^*(k_i), p_i^*(k_i))\}$ obtained from the DESRA algorithm, there is no other control sequence that fulfills this condition. This is in contradiction with the feasibility of the demand sequence from Definition 2. Hence, condition (13) is met for all movements $j \in \mathcal{J}_{\mathrm{in}} \cup \mathcal{J}_{\mathrm{E}}$, and this concludes the proof of the theorem. □

Remark 2. The network stability condition defined in the max-pressure algorithm papers (Wongpiromsarn et al., 2012; Varaiya, 2013) states that the queuing process $X(t) = \{x_{ji}(t) | x_{ji}(t) = q_{ji}^{\mathrm{arr}}(k_i)p_i(t) - F_{ji}(\mathcal{P}_i, t)\}$ is stable in the mean over time period $[0, T]$, if there exists a constant $K < \infty$ such that the following inequality holds:

$$1/T \sum_{t=0}^{T} \sum_{i} \sum_{j \in \mathcal{J}_i} x_{ji}(t) < K \tag{14}$$

The α-stability condition defined in Definition 1 is less conservative than this stability condition from two perspectives: (i) Condition (14) only implies the boundedness of the average queue sizes, while their upperbounds could be arbitrarily large, and (ii) the max-pressure stability definition entails a boundedness condition for the sum of the queue sizes of the whole network, rather than the queue size boundedness of every link across the network that is enforced via Definition 1.

Remark 3. The admissible demand sequence $\{q_l^{\mathrm{E}}(t)\}$ ($l \in \mathcal{J}_{\mathrm{E}}$ and $t \in [0, T]$) defined in Varaiya (2013) is a demand for which there exists a control sequence $\{(\lambda_{ji}(t), p_i(t))\}$ and a constant $\xi > 0$, such that for every movement j at each intersection i the following inequality holds:

$$\sum_{t=1}^{T} \left(q_{ji}^{\mathrm{arr}}(t)p_i(t) - F_{ji}(\mathcal{P}_i, t) \right) < -\xi T. \tag{15}$$

Comparing inequalities (13) and (15), it can be interpreted that the amenable demand defined in Definition 2 is less conservative than this definition, as Definition 2 permits a level of oversaturation at the intersection over the whole control period. However, Inequality (15) implies that every movement in the network must be strictly undersaturated.

Let us define $Q_{ji}(t)$ ($j \in \mathcal{J}_i$, $i \in \{1, \dots, I\}$) as the queue size of movement j at intersection i at time $t \geq 0$, and $Q(t) = [Q_{ji}](t)$ as the vector of queue sizes in the network. The α-stability concept ensures the robust stability of the traffic network under bounded and admissible disturbances $\{q_j^{\mathrm{E}}(t)\}$, $j \in \mathcal{J}_{\mathrm{E}}$. In other words, the DESRA algorithm ensures that the queue sizes $Q_{ji}(t)$ throughout the network remain *bounded* and *less than or equal to* the link's storage capacity. We next employ the passivity theory to prove that when there is no external flows into the network, i.e. when $\{q_j^{\mathrm{E}}(t)\} \equiv 0$, all the accumulated queues asymptotically discharge with time. It means that for each movement j at every intersection i, $Q_{ji}(t)$ approaches to zero as time grows ($t \to \infty$). This is called the *asymptotic stability* of the zero dynamics of the controlled traffic network. Passivity (defined below) is a stability concept introduced for network control systems, indicating that a complex dynamic network is robust stable if the net increase in the internal energy of the network is essentially bounded. A passive system is also dissipative, i.e. it consistently dissipates energy.

Definition 3 (*Byrnes et al., 1991*)**.** A dynamic system with states $\mathbf{x}(t)$, inputs $\mathbf{u}(t)$ and outputs $\mathbf{y}(t)$ is passive in $[t_1, t_2]$ if there exists an storage function (a non-negative function) $V(x(t))$ such that

$$\int_{t_1}^{t_2} \mathbf{u}^T(t)\mathbf{y}(t)\mathrm{d}t \geq V(x(t_2)) - V(x(t_1)). \tag{16}$$

The expression $\mathbf{u}^T(t)\mathbf{y}(t)$ is the supply rate of the network. In our transport network problem, the output $\mathbf{y}(t)$ is the vector of queue sizes of the movements at the intersections $[Q_{ji}](t)$ ($j \in \mathcal{J}_i$, $i \in \{1, \dots, I\}$). Moreover, the control input $\mathbf{u}(t)$ can be interpreted as the vector of effective outflow rates $[F_{ji}(\mathcal{P}_i, \cdot)/(G_i(\mathcal{P}_i, \cdot) + L_i(\cdot))](t)$ that are defined at discrete events $t = t(k_i)$. As such, $\mathbf{u}^T(k_i)\mathbf{y}(k_i) = \sum_i \sum_{j \in \mathcal{J}_i} F_{ji}(\mathcal{P}_i, k_i)Q_{ji}(k_i)/(G_i(\mathcal{P}_i, k_i) + L_i(k_i))$ that represents the supply rate of the whole network in [veh^2/h]. To add, we define the storage function as $V(Q(t)) = \sum_i \sum_{j \in \mathcal{J}_i} Q_{ji}^2(t)$. Since $V(0) = 0$ and $V(Q(t)) \geq 0$, it can be shown via Lyapunov theory that if the traffic network is passive, then its zero dynamics is asymptotically stable (Byrnes et al., 1991). Note that the passivity of the network is shown given bounded external disturbances (i.e. the inflows to the network $\{q_j^{\mathrm{E}}(t)\}$), which itself is an indicator of robust stability of the controlled network.

Based on the shockwave theory and the DESRA algorithm, the queue size dynamics of the controlled system without restricting its upper-bound to the link length can be formulated as follows:

$$\begin{aligned} Q_{ji}(k_i + 1) = \quad & Q_{ji}(k_i) + \max\{-Q_{ji}(k_i), ((\Gamma_{ji}(k_i) - 1)Q_{ji}(k_i) - G_i^{\min}(\mathcal{P}_i^*, k_i)S_{ji} \\ & + \tilde{\Gamma}_{ji}(k_i)L_i)\lambda_{ji}(k_i) + \left(\tilde{\Gamma}_{ji}(k_i)(G_i^{\min}(\mathcal{P}_i^*, k_i) + L_i(k_i))\right)(1 - \lambda_{ji}(k_i))\} \end{aligned} \tag{17}$$

where $\Gamma_{ji}(k_i) = \dfrac{\kappa_{ji}^{\mathrm{cri}}(\kappa_{ji}^{\mathrm{jam}} - \kappa_{ji}^{\mathrm{arr}}(k_i))}{\kappa_{ji}^{\mathrm{jam}}(\kappa_{ji}^{\mathrm{cri}} - \kappa_{ji}^{\mathrm{arr}}(k_i))}$, $\tilde{\Gamma}_{ji}(k_i) = \dfrac{\kappa_{ji}^{\mathrm{cri}} q_{ji}^{\mathrm{arr}}(k_i)}{\kappa_{ji}^{\mathrm{cri}} - \kappa_{ji}^{\mathrm{arr}}(k_i)}$.

Now, we prove the passivity, and thus the asymptotic stability of the traffic network controlled by the DESRA algorithm.

Theorem 2. *The signalized traffic network controlled by the DESRA algorithm is passive over time period* $[0, T]$*, if the network's demand is admissible in the sense of Definition 2.*

Proof. According to Definition 3 it is sufficient to show the following inequality

$$\sum_i \sum_{j\in\mathcal{J}_i} \int_0^T \frac{F_{ji}(\mathcal{P}_i,t)Q_{ji}(t)}{G_i(\mathcal{P}_i,t)+L_i(t)}\mathrm{d}t \geq \sum_i \sum_{j\in\mathcal{J}_i} \left(Q_{ji}^2(T)-Q_{ji}^2(0)\right). \tag{18}$$

In light of that, we find a lower bound of the right-hand-side of (18). Similar to the proof of Theorem 1, only the optimal phase $\mathcal{P}_i^*(k_i)=\mathcal{P}_{i,\mathrm{Iter1}}^*(k_i)$ is considered in the analysis, and additional movements appended in the phase improvement step further increase the passivity of the network. By applying the DESRA control algorithm, the left-hand-side of (18) can be written as

$$\sum_i \sum_{j\in\mathcal{J}_i} \int_0^T \frac{F_{ji}(\mathcal{P}_i,t)Q_{ji}(t)}{G_i(\mathcal{P}_i^*,t)+L_i(t)}\mathrm{d}t \approx \sum_{k_i}\sum_i \sum_{j\in\mathcal{M}_{p_i}} \frac{G_i^{\min}(\mathcal{P}_i^*,k_i)S_{ji}}{G_i^{\min}(\mathcal{P}_i^*,k_i)+L_i(k_i)}Q_{ji}(k_i)\geq 0. \tag{19}$$

Let us define $V_i(k_i)=\sum_{j\in\mathcal{J}_i}Q_{ji}^2(k_i)$. Based on Eq. (17), the storage function's difference equation can be written as

$$\begin{aligned}\textstyle\sum_i V_i(k_i+1)-V_i(k_i) &= \textstyle\sum_i\sum_{j\in\mathcal{J}_i} Q_{ji}^2(k_i+1)-Q_{ji}^2(k_i)\\ &= \textstyle\sum_i\sum_{j\in\mathcal{J}_i}\left\{(\Gamma_{ji}(k_i)-1)Q_{ji}(k_i)-G_i^{\min}(\mathcal{P}_i^*,k_i)S_{ji}+\tilde{\Gamma}_{ji}(k_i)L_i(k_i)\right\}^2\lambda_{ji}^*(k_i)\\ &+\left\{\tilde{\Gamma}_{ji}(k_i)(G_i^{\min}(\mathcal{P}_i^*,k_i)+L_i(k_i))\right\}^2(1-\lambda_{ji}^*(k_i))\\ &+2Q_{ji}(k_i)\left\{(\Gamma_{ji}(k_i)-1)Q_{ji}(k_i)-G_i^{\min}(\mathcal{P}_i^*,k_i)S_{ji}+\tilde{\Gamma}_{ji}(k_i)L_i(k_i)\right\}\lambda_{ji}^*(k_i)\\ &+2Q_{ji}(k_i)\left(\tilde{\Gamma}_{ji}(k_i)(G_i^{\min}(\mathcal{P}_i^*,k_i)+L_i(k_i))\right)(1-\lambda_{ji}^*(k_i)).\end{aligned} \tag{20}$$

Since the queue size of movements with the right-of-way at intersection i decreases, it can be shown that there exist $\epsilon_{ji}<1$, such that

$$-Q_{ji}(k_i)\leq(\Gamma_{ji}(k_i)-1)Q_{ji}(k_i)-G_i^{\min}(\mathcal{P}_i^*,k_i)S_{ji}+\tilde{\Gamma}_{ji}(k_i)L_i\leq-\epsilon_{ji}Q_{ji}(k_i) \tag{21}$$

Moreover, since the demand is admissible and thus the network is α-stable, the queue size of each link does not exceed the storage capacity of the link, i.e.

$$0\leq\tilde{\Gamma}_{ji}(k_i)(G_i^{\min}(\mathcal{P}_i^*,k_i)+L_i)\leq\Delta_{ji}K_{ji}^{\mathrm{jam}}-Q_{ji}(k_i) \tag{22}$$

Therefore, from (20), (21), and (22), one gets

$$\sum_i V_i(k_i+1)-V_i(k_i)\geq-\sum_i\sum_{j\in\mathcal{M}_{\mathcal{P}_i}^*}(2-\epsilon_{ji}^2)Q_{ji}^2(k_i)\geq-\sum_i\sum_{j\in\mathcal{M}_{\mathcal{P}_i}^*}\tilde{\epsilon}_{ji}Q_{ji}^2(k_i), \tag{23}$$

where $\tilde{\epsilon}_{ji}>0$ is a scalar constant. Hence, since $V(T)-V(0)=\sum_i\sum_{k_i}V_i(k_i+1)-V_i(k_i)$, inequality below can be derived from (23)

$$V(T)-V(0)\geq-\sum_{k_i}\sum_i\sum_{j\in\mathcal{M}_{\mathcal{P}_i}^*}\tilde{\epsilon}_{ji}Q_{ji}^2(k_i). \tag{24}$$

It is clear from (19) and (24) that Inequality (18) is fulfilled and this concludes the proof of the theorem. □

4.2. Notes on the optimality of the DESRA algorithm

In this section we show that under a certain homogeneity condition of the traffic network, the DESRA algorithm maximizes the sum of intersections' throughput. Let us define $q_{ji}^{\mathrm{out}}(t)$ as the effective outflow of movement j at intersection i. The following theorem summarizes the main finding of this section.

Theorem 3. *The DESRA algorithm maximizes the total throughput of all intersections in the network over time period* $[0,T]$*, if and only if for each time* $t\in(t(k_i),t(k_i)+G_i^{\min}(\mathcal{P}_i^*(k_i),k_i))$ *and for every phase* $\mathcal{P}_i\neq\mathcal{P}_i^*(k_i)\in\Phi_i$ *the following inequality holds*

$$\sum_{j\in\mathcal{M}_{\mathcal{P}_i}}\frac{G_i'(\mathcal{P}_i,t)S_{ji}}{G_i'(\mathcal{P}_i,t)+L_i(t)}\leq\sum_{j\in\mathcal{M}_{\mathcal{P}_i^*}}\frac{G_i^{\min}(\mathcal{P}_i^*,k_i)S_{ji}}{G_i^{\min}(\mathcal{P}_i^*,k_i)+L_i(k_i)}, \tag{25}$$

where $G_i'(\mathcal{P}_i,t)=\min_{j\in\mathcal{M}_{\mathcal{P}_i}}G'^{\mathrm{sat}}_{ji}(k_i)$.

Proof. We show that upon fulfillment of Condition (25) the DESRA algorithm optimizes the throughput of every intersection in the network, and thus maximizes the total throughput of the network. Total throughput at intersection i under a generic control sequence $\{(\lambda_{ji}(k_i),p_i(k_i))\}$ can be formulated as follows:

$$\begin{aligned}\textstyle\sum_{j\in\mathcal{M}_{\mathcal{P}_i}}\int_0^T q_{ji}^{\mathrm{out}}(t)\mathrm{d}t &= \textstyle\sum_{k_i}\sum_{j\in\mathcal{M}_{p_i}} q_{ji}^{\mathrm{out}}(k_i)G_i(\mathcal{P}_i,k_i)\\ &= \textstyle\sum_{k_i}\sum_{j_1\in\mathcal{M}_{\mathcal{P}_i}} S_{j_1i}G_i(\mathcal{P}_i,k_i)\\ &+\textstyle\sum_{k_i}\sum_{j_2\in\mathcal{M}_{\mathcal{P}_i}}\left(S_{j_2i}G_{j_2i}^{\mathrm{sat}}(k_i)+q_{j_2i}^{\mathrm{arr}}(k_i)\left(G_i(\mathcal{P}_i,k_i)-G_{j_2i}^{\mathrm{sat}}(k_i)\right)\right)\\ &+\textstyle\sum_{k_i}\sum_{j_3\in\mathcal{M}_{\mathcal{P}_i}} S_{j_3i}G_{j_3i}^{\mathrm{sat}}(k_i),\end{aligned} \tag{26}$$

where j_1, j_2, and j_3 are movements in $\mathcal{M}_{\mathcal{P}_i}$ wherein $G_i(\mathcal{P}_i,k_i) \le G^{\text{sat}}_{j_1 i}(k_i)$; $G_i(\mathcal{P}_i,k_i) > G^{\text{sat}}_{j_2 i}(k_i)$ and $x^{\text{M}}_{j_2 i}(k_i) \le x^{\text{d}}_{j_2 i}(k_i)$; and $G_i(\mathcal{P}_i,k_i) > G^{\text{sat}}_{j_3 i}(k_i)$ and $x^{\text{M}}_{j_3 i}(k_i) > x^{\text{d}}_{j_3 i}(k_i)$, respectively. It is clear that the right-hand-side of (26) is maximized by selecting phase $\mathcal{P}^*_i$ and green time $G^{\min}_i(\mathcal{P}^*_i,k_i)$ at time $t = t(k_i)$ (as every movement in $\mathcal{M}_{\mathcal{P}^*_i}$ belongs to class j_1), which is achieved via the DESRA scheme. Moreover, if Condition (26) is satisfied, then the effective outflow at the intersection and thus the throughput is also maximized for every time t between $t(k_i)$ and $t(k_i) + G^{\min}_i(\mathcal{P}^*_i(k_i),k_i)$. Thereby, Condition (26) is a sufficient condition for the optimality of the DESRA algorithm. In addition, if Condition (26) is not satisfied, then there exists a time interval within $(t(k_i), t(k_i) + G^{\min}_i(\mathcal{P}^*_i(k_i),k_i))$ in which the effective outflow is maximized by activating a phase $\mathcal{P}_i$ other than $\mathcal{P}^*_i(k_i)$. Hence, Condition (26) is also a necessary condition for the optimality of the DESRA algorithm, and this concludes the proof of the theorem. □

Theorem 3 implies that if the sum of saturation flows of movements of all phases at the intersection are in a similar range, then the DESRA algorithm maximizes the total throughput of all the network intersections. However, if for example one phase, $\tilde{\mathcal{P}}_i \in \boldsymbol{\Phi}_i$, has considerably greater effective outflow rate with respect to other possible phases at intersection i, then soon after the phase receives the red time and queues are accumulated at its movements (say time $\tilde{t}_i$), it becomes the optimal phase again in maximizing the throughput at the intersection. The time $\tilde{t}_i$ could be less than the green time allocated to the phase that is activated after $\tilde{\mathcal{P}}_i$. In such a circumstance, the DESRA scheme is not optimal in maximizing the throughput.

5. Microsimulation results and discussion

In this section, we conduct microsimulation experiments and provide a comprehensive quantitative evaluation by comparing our proposed DESRA method with two benchmark methods, including a fixed-time signal control, based on the Webster method (Webster, 1958), and the actuated signal control. The fixed signal timing in the Webster method is determined based on the average traffic demand during the study period. However, in the actuated traffic signal control method (which we call Actuated method in short form), traffic signal timing is continuously adjusted in response to real-time measures of traffic obtained from detectors installed on all the approaches. Different detectors are used to distinguish different movements (on lanes). By receiving a call from detectors, the Actuated controller, based on some pre-defined thresholds, decides whether to extend or terminate the green phase in response to the actuation source. Although the Actuated method has a better performance than the fixed-time method in most cases, it does not offer any real-time optimization to adapt to traffic fluctuations and possible spillbacks properly. Some of the Actuated method's parameters used in this paper are: (i) distance of detectors from the stoplines = 20 (m), (ii) minimum green time = 7 (s), (iii) maximum green time = 53 (s), and (iv) extension time = 3 (s).

5.1. Experiment setup

The experiments are conducted in AIMSUN microsimulation environment. To evaluate the proposed DESRA framework, two cases are studied: (i) an isolated intersection and (ii) a 5 × 5 network comprising 25 intersections. In both cases, a typical 4-approach intersection is considered, in which each approach consists of three lanes with distinct movements, including left-turn, through, and right-turn lanes, as shown in Fig. 6a. The movements are ordered from 1 to J counterclockwise, starting at eastbound left-turn. The total number of movements in an intersection, J, is 12. Moreover, the maximum number of simultaneously non-conflicting movements in a phase is 4, and the total number of identified possible phases, is 111. The possible phases include 12 one-movement, 38 two-movement, 44 three-movement, and 17 four-movement phases. It is worth mentioning that coordination (e.g. green wave) is one measure to avoid spillbacks; nevertheless, without an explicit coordination mechanism it is still possible to avoid spillbacks. To have a deeper investigation of the performance of our method compared to a method involving coordination, we additionally conducted a corridor experiment, which is briefly presented in Appendix C.

In the isolated intersection test case, all approaches are equally 300 (m) long. A 2.5-hour time-varying demand scenario is employed, as depicted in Fig. 6b. Thirty simulation replications are run with various random seeds with a 30-minute warm-up period at the beginning of each experiment.

In the network case, 20 external centroids at the outer links are used to generate and attract trips. In addition, 25 generative-only internal centroids are also designed to feed the network internally, which operate similar to side streets. The length of all internal links in the network is set to 350 (m). The network case study is evaluated with two different demand levels, medium and high, in 2-hour time-varying demand scenarios, see Fig. 6c and d. Ten simulation replications are run with a 15-minute warm-up period.

Saturated green time is a key component in our proposed method, see Section 3.1. It is estimated based on queue lengths, arrival flow data, and FD. In both isolated and network cases, queue lengths are estimated by counting the number of stopped vehicles in each lane and multiplying it in 1 over $\mathcal{K}^{\text{jam}}_{ji}$. Stopped vehicles are defined as vehicles with a speed that is lower or equal to 5 (km/h). During a high traffic load in the network, where recognizing the end of the queue is crucial, we use the position of the last stopped vehicle, as the end of the queue. In the simulation setup, the initial queue length is read through AIMSUN software; however, in real-world applications, this data can be collected through different methods such as traffic cameras, detectors, and probe data.

In the network case, the arrival flow estimation method described in Appendix B is employed. For this purpose, a detector at the beginning of each link is installed to read the count of vehicles in each 10 s interval and follow the arrival flow estimation process. It is assumed that the estimated arrival flow is distributed equally among the three movements (i.e., 1/3 for each lane). The presented arrival flow estimation method for the network case in Appendix B is also applicable in the case of the isolated intersection.

The traffic signal control requires FDs; hence, we simulated 30 replications to determine three FDs for each type of movement, including left, through, and right turns. In Fig. 7, the FD for right turns is depicted as a sample. The extracted triangular FD parameters for different movements are provided in Table 1.

It should be noted that all tests include en-route dynamic traffic assignment. Moreover, yellow time and lost time are considered as 3 (s) and 4 (s), respectively.

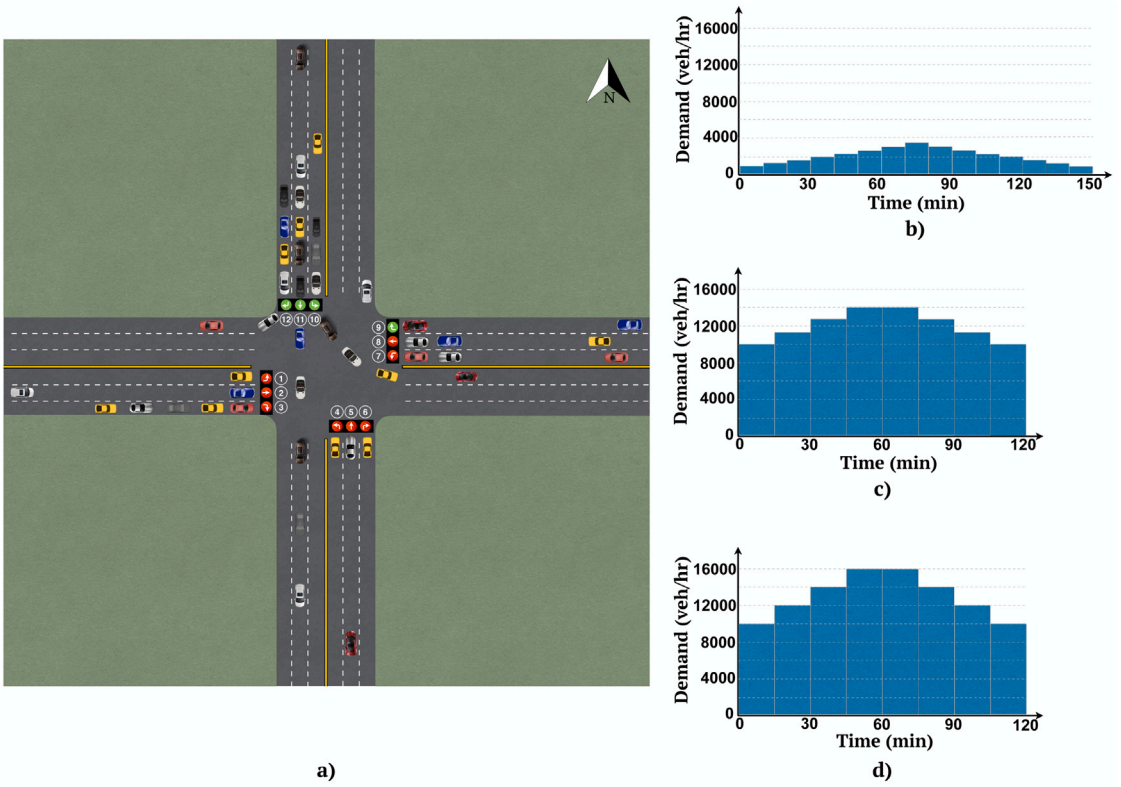

Fig. 6. A typical intersection and traffic demands of microsimulation case studies: (a) An intersection with four incoming and four outgoing approaches, where each approach includes three distinct left-turn, through, and right-turn lanes, (b) total demand to all approaches in the isolated intersection test case, (c) medium demand in the network test case, and (d) high demand in the network test case.

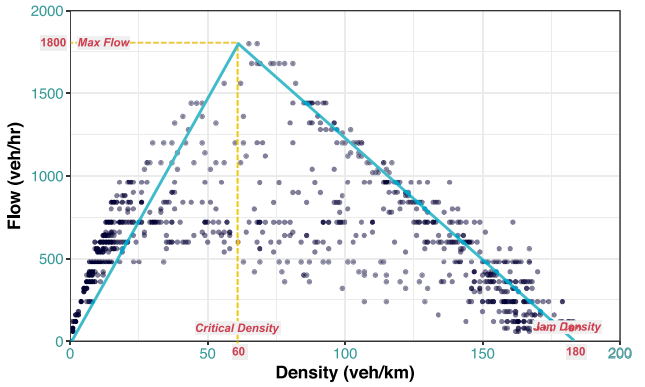

Fig. 7. A sample triangular FD for the right turns estimated in an offline process: the extracted parameters are S = 1800 (veh/h), $\mathcal{K}^{cri}$ = 60 (veh/km), $\mathcal{K}^{jam}$ = 180 (veh/km), u^a = 30 (km/h).

Table 1
Extracted FD parameters for the three types of movements.

Movement	S (veh/h)	$\mathcal{K}^{cri}$ (veh/km)	$\mathcal{K}^{jam}$ (veh/km)	u^a (km/h)
Left turn	1650	55	180	30
Through	2200	55	180	40
Right turn	1800	60	180	30

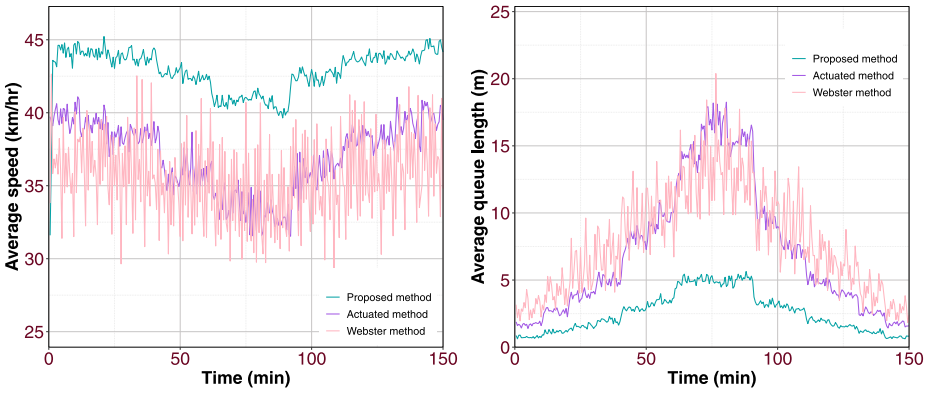

(a) (b)

Fig. 8. Comparison of (a) average speed, and (b) average queue length, in each 30 (s) interval over 2.5 (h).

Table 2
Comparison of the three methods in isolated intersection case. The numbers in parentheses show the improvements in terms of % with respect to the Webster method.

	Proposed method	Actuated method	Webster method
Average travel time (sec/km)	87.9 (25.7%)	114.2 (3.5%)	118.3
Average speed (km/h)	42.4 (22.5%)	35.7 (3.2%)	34.6

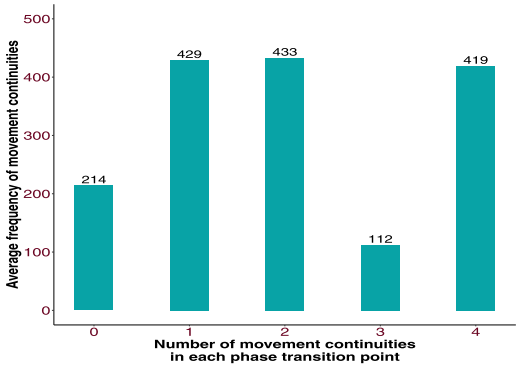

Fig. 9. Average frequency of movement continuities between two successive phases in the isolated test case with the proposed method.

5.2. Isolated intersection case study

First, we study the isolated intersection test case. Results are shown in Fig. 8 where the average speed and average queue length during every 30 s are plotted over time. Using the proposed DESRA algorithm, the average speed increases 18.8% and 22.5% compared to the Actuated method and Webster method, respectively (see Table 2). Average travel time has been reduced by 23.0% and 25.7% compared to the Actuated and Webster methods, respectively.

In Fig. 8b, we observe that the DESRA scheme is more efficient than other methods in reducing the average queue length considered over all lanes of the intersection. As shown in Fig. 8b, the DESRA scheme controls the average queue lengths under 6 (m) while the average queue lengths in Actuated and Webster methods range from 2 (m) to 18 (m), and 2 (m) to 20 (m), respectively. In other words, a maximum of 12 vehicles are in all approaches during the experiments on average using the DESRA algorithm, while with the Actuated and Webster methods, this increases to 36 and 40 vehicles, respectively. These comparisons indicate that the proposed method is more efficient than the two other methods to control the isolated traffic signal.

Fig. 9 demonstrates that during the 2.5-hour experiment, 3307 movements out of the total of 6428 activated movements are prevented from unnecessary signal switches from green to yellow. This accounts for 51.4% of total activated movements, which have a significant impact on the intersection performance. This is achieved as a result of considering and maintaining the movement continuity between successive phases in the phase improvement stage, which was explained in Section 3.4. Note that consideration for movement continuity is a byproduct of acyclic phases in which a movement can be repeated over several successive phases.

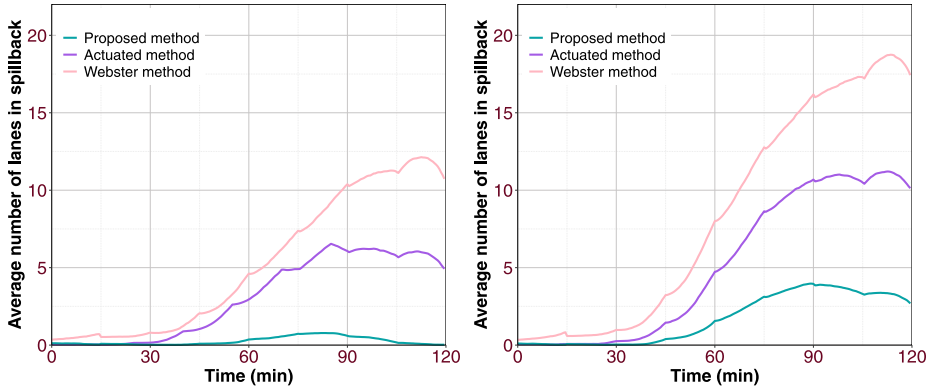

(a) Medium demand (b) High demand

Fig. 10. Average number of lanes in spillback in the network with (a) medium demand and (b) high demand.

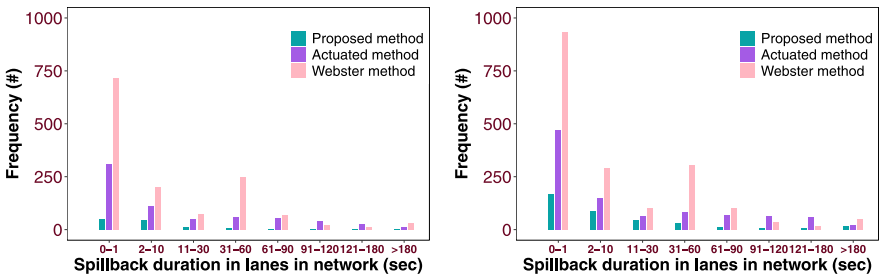

(a) Medium demand (b) High demand

Fig. 11. Frequency of spillback duration in lanes in the network with (a) medium demand and (b) high demand.

5.3. Network case study

Here, an experiment is performed to evaluate the effectiveness of the proposed DESRA algorithm in the network settings. In this experiment, spillback control is integrated into the methodology. The results in Fig. 10 indicate the improved performance of the DESRA algorithm in reducing the number of spillbacks in the lanes in the network with both medium and high demands. With medium demand, the proposed method clears all spillbacks in lanes while the average number of lanes with spillback at the end of simulation in Actuated and Webster methods are 5 and 11, respectively. These numbers for the high demand for the proposed, Actuated, and Webster methods are 2.5, 10, and 17.5, respectively.

We also studied the impact of the three methods on the length and frequency of spillbacks at the lane level in the network for both medium and high demands. Eight different ranges of spillback duration were considered. Results shown in Fig. 11 clearly support the efficiency of the proposed method in reducing the time and frequency of the spillbacks in the network. In all ranges of spillback durations, the frequency of spillbacks with the proposed method is less than the two other methods for both medium and high demands.

Comparison of network macroscopic fundamental diagrams (MFDs) of the network with the three control methods with both medium and high traffic demands show a higher production of the network when the proposed DESRA framework is applied (see Figs. 12a and 12b). Additionally, the proposed control methodology prevents the network from experiencing the congested regime.

Results depicted in Figs. 13a and 13b for the average speed and 13c and 13d for the average queue length in the network also confirm the effectiveness of the proposed method. Average speed in the network using the proposed method is 19 (km/h) with the medium demand (ignoring the data for the first minute) and 14 (km/h) with the high demand. However, the average speed falls down to about 9 (km/h) with the medium demand and 7 (km/h) with the high demand using both two other signal control methods. Moreover, the average queue length in the network with medium demand peaks at 19 (m), 55 (m), and 75 (m) using the proposed, Actuated, and Webster method. For the high demand, the maximum of average queue length using the proposed, Actuated, and Webster method are 38 (m), 83 (m), and 103 (m), respectively. Average travel time with the proposed DESRA scheme in medium and high traffic demands are 43.3% and 37.7% lower than the Actuated method, respectively. Compared to the Webster method, these reductions are 52.9% and 46.4%, respectively (see Table 3).

The distributions of green time duration in all replications for the proposed and Actuated methods are shown in Figs. 14a and 14b. The green times are limited to the range of 7 to 53 (s) in the Actuated method, whereas, as depicted, the proposed method provides

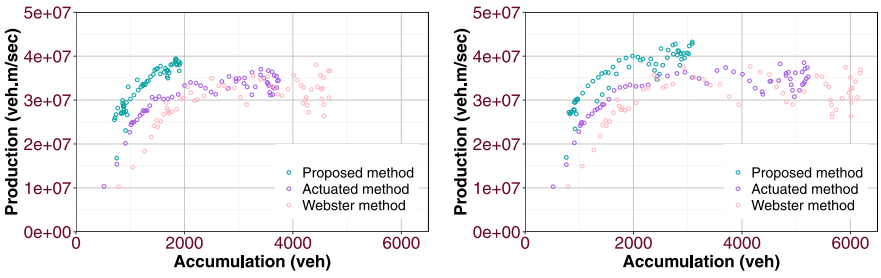

(a) Medium demand (b) High demand

Fig. 12. MFD of the network with (a) medium demand, and (b) high demand.

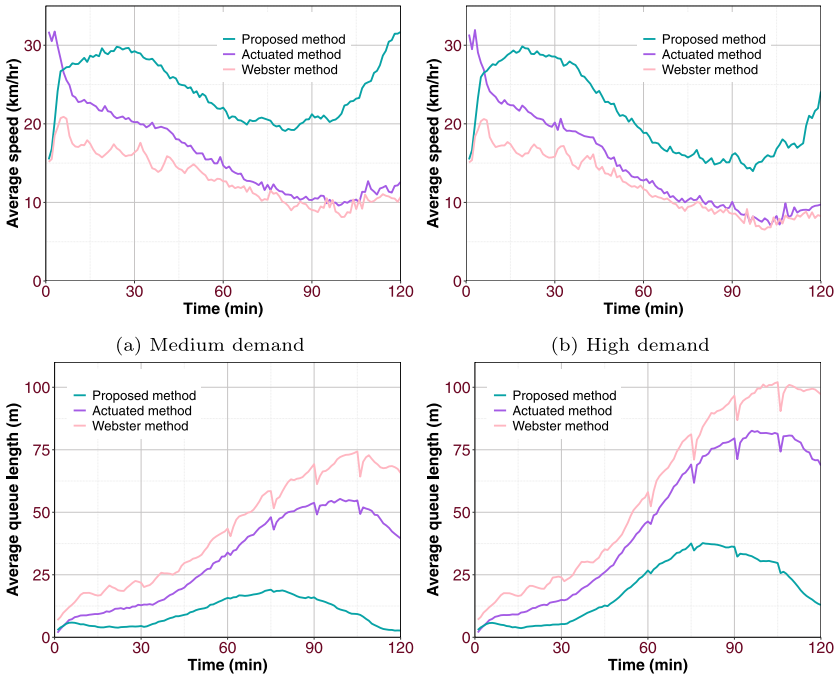

(a) Medium demand (b) High demand

(c) Medium demand (d) High demand

Fig. 13. Comparison of average speed and average queue length in the network over 120 min: (a) average speed (medium demand), (b) average speed (high demand), (c) average queue length (medium demand), and (d) average queue length (high demand).

Table 3
Comparison of the three methods in the network case. The numbers in parentheses show the improvements in terms of % with respect to the Webster method.

	Demand level	Proposed method	Actuated method	Webster method
Average travel time (sec/km)	Medium	136.0 (52.9%)	239.6 (17.0%)	288.6
	High	176.1 (46.4%)	282.6 (14.1%)	328.8
Average speed (km/h)	Medium	29.0 (90.8%)	18.3 (20.4%)	15.2
	High	24.7 (73.9%)	16.7 (17.6%)	14.2

a wider range of green times compared to the Actuated method. The maximum green times of a movement in the proposed method for medium and high demands are 249 (s) and 411 (s), respectively. Evidently, with higher traffic demand, the green times required to accommodate the traffic increases, which is confirmed by the performance of the proposed DESRA algorithm. Note that one movement may remain active for 249 s over several phases, while the other simultaneous non-conflicting movements may change during the 249 s. Furthermore, the minimum green time is 2 (s) for both medium and high demand. Although the proposed method provides a broader range of green times, the average of green time durations in the proposed method for medium and high demands are 13.9 and 16.1 (s) lower than the average green times in the Actuated method which are 29.6 and 31.8 (s), respectively. The

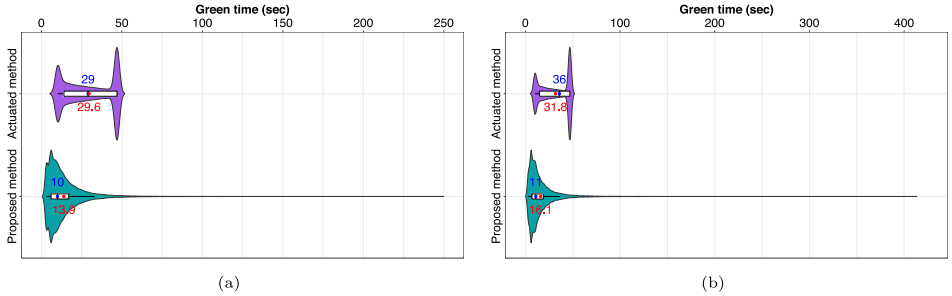

Fig. 14. Comparison of green times between the proposed method and Actuated method in the network with (a) medium demand and (b) high demand.

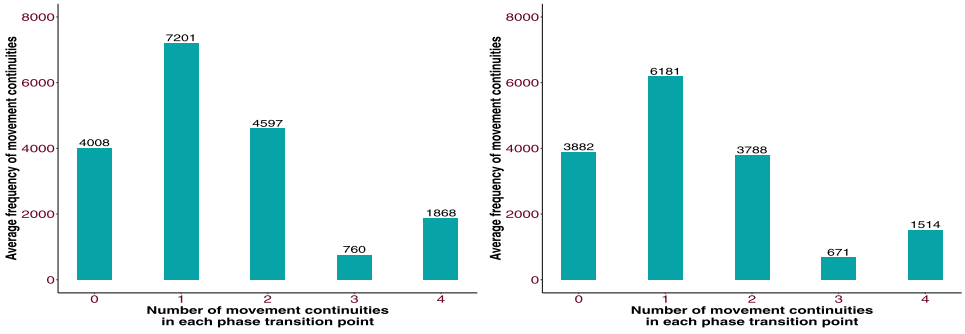

Fig. 15. Average frequency of movement continuities between two successive phases in phase transition points in the network with the proposed method.

shorter green time in the proposed method reflects shorter red times for conflicting movements, and hence provides less probability of spillback.

Figs. 15a and 15b show a large number of times that yellow phase can be avoided by the proposed method. During a 2-hour experiment, 26 147 movements out of the total of 73 736 activated movements of medium demand and 21 826 movements out of the total of 64 144 activated movements of high demand were prevented from unnecessary signal switches from green to yellow. These numbers account for 35.5% and 34.0% of total activated movements, which are considerable portions of the activated movements and have a significant impact on the network performance reducing the extent of acceleration and deceleration of platoons of vehicles.

6. Summary and future research

In this paper, we have proposed a real-time decentralized traffic signal control method for urban networks called DESRA. The proposed method is acyclic and based on lane-based queue measurements. There is no communication between intersections and all control decisions in the network are entirely local. Each intersection is independently controlled based on estimated arrival flow and queue length at the end of the previous time step collected in all lanes of the intersection. The control decisions for each intersection in the network include phase time, active movements in the phase, and interphase.

Furthermore, a new stability concept has been introduced for the network-level traffic, and the robust stability and asymptotic stability of the traffic network have been verified. Moreover, it has been shown that under certain conditions the DESRA algorithm optimally maximizes the total throughput of the network intersections.

In brief, the method first finds the minimum saturated green time in all possible phases. This is to guarantee that vehicles discharge at their full capacity during a phase. In determining the minimum saturated green time, a spillback control is also applied, which considers the impact of the storage capacity of the downstream links on the control decisions. Then, the estimated effective outflow rate during the minimum saturated green time of each phase is obtained, and the phase and phase time with maximum estimated effective outflow rate is determined. Without changing the selected phase time, the process of phase improvement is done to increase the outflow of the intersection by increasing the number of active movements in the selected phase and prioritizing longer queues. Lastly, based on the selected ideal phase and previous phase, the interphase is determined to facilitate movement continuity.

Using microsimulation, we compared our DESRA algorithm against other well-known benchmark methods (Actuated and Webster methods) from different aspects, including average speed, average queue length, and average travel time in both isolated and network scenarios. In addition, we mainly evaluated our method in the network case in terms of frequency of lane spillbacks and MFD of the

network. The results showed that our proposed method outperforms benchmark methods, fixed time and actuated signal control, in cases of both isolated intersection and network.

For future work, the proposed network control methodology can be studied in conjunction with a route recommendation system (Chow et al., 2020). Enhancing the algorithm by incorporating it within a hierarchical control scheme such as Perimeter control (Li et al., 2021; Sirmatel and Geroliminis, 2021) is another future direction. The impact of link length and noise in the queue length and arrival flow estimations can also be studied. Considering lanes with mixed movements is also an extension of this work. Furthermore, other elements of traffic such as transit priority, Emergency Medical Services (EMS) priority, and multi-modality can be considered to provide a comprehensive method as a solution for a complex city-scale network.

CRediT authorship contribution statement

Mohammad Noaeen: Conceptualization, Methodology, Software, Validation, Formal analysis, Investigation, Data curation, Writing – original draft, Writing – review & editing. **Reza Mohajerpoor:** Methodology, Formal analysis, Writing – original draft. **Behrouz H. Far:** Methodology, Formal analysis, Writing – original draft, Supervision. **Mohsen Ramezani:** Conceptualization, Methodology, Validation, Formal analysis, Investigation, Writing – original draft, Writing – review & editing, Supervision.

Appendix A. Nomenclature

Notation	Description
j	Traffic movements, $j \in \{1, 2, \dots, J_i\}$
J_i	Total number of movements at intersection i, for the defined test case $J_i = 12$
$\mathcal{J}_i$	The set of traffic movements at intersection i
i	Index of intersections, $i \in \{1, 2, \dots, I\}$
I	Total number of intersections
$\boldsymbol{\Phi}_i$	Set of all possible phases at intersection i
k_i	Discrete time index at intersection i, $k_i \in \{0, 1, \dots\}$
λ_{ji}	Signal indications (0 for red and 1 for green signal indication) of movement j at intersection i
$\mathcal{P}_i(k_i)$	A possible phase at intersection i at time-step k_i
$t(k_i)$ (unit of time)	Phase transition point
$p_i(k_i)$ (unit of time)	Phase time at intersection i at time-step k_i
$\mathcal{I}_i(k_i)$	Interphase of intersection i at time-step k_i
$\psi^*(k_i)$	Ideal phase at time-step k_i
$G_{ji}^{\text{sat}}(k_i)$ (unit of time)	Saturated green time of movement j at intersection i at time-step k_i assuming that there is insufficient storage capacity at the downstream link of movement j
$G_{ji}^{\text{s}}(k_i)$ (unit of time)	Saturated green time of movement j at intersection i at time-step k_i assuming that there is sufficient storage capacity at the downstream link of movement j
$\mathcal{K}_{ji}^{\text{jam}}$ (veh/unit of distance)	Jam density of movement j at intersection i
S_{ji} (veh/unit of time)	Saturation flow of movement j at intersection i
$x_{ji}^{0}(k_i)$ (unit of distance)	Queue length in movement j at intersection i at time-step k_i
$\mathcal{K}_{ji}^{\text{arr}}$ (veh/unit of distance)	Arrival density of movement j at intersection i
$q_{ji}^{\text{arr}}(k_i)$ (veh/unit of time)	Arrival flow of movement j at intersection i at time-step k_i
$\mathcal{K}_{ji}^{\text{cri}}$ (veh/unit of distance)	Critical density of movement j at intersection i
$SWI_{ji}(k_i)$ (unit of distance/unit of time)	Backward-moving estimated shockwave formed between arriving vehicles and queued vehicles for movement j at intersection i at time-step k_i
$SWR_{ji}(k_i)$ (unit of distance/unit of time)	Backward-moving estimated shockwave formed between queued vehicles and vehicles leaving queue at saturation for movement j at intersection i at time-step k_i
$SWN_{ji}(k_i)$ (unit of distance/unit of time)	Forward-moving estimated shockwave formed between arriving vehicles and vehicles leaving queue at saturation for movement j at intersection i at time-step k_i
Δ_{ji} (unit of distance)	Link length of movement j at intersection i
$x_{ji}^{\text{M}}(k_i)$ (unit of distance)	Maximum queue extent in movement j at intersection i at time-step k_i
$G_{ji}^{\text{d}}(k_i)$ (unit of time)	Available time capacity of the link downstream of movement j at time-step k_i
$x_{ji}^{\text{d}}(k_i)$ (unit of distance)	Available storage capacity of the link downstream of movement j at time-step k_i
Δ_{ji}^{d} (unit of distance)	Link length of the lane downstream of movement j at intersection i
$x_{ji}^{\text{0dL}}(k_i)$ (unit of distance)	Maximum queue length of the lane downstream of movement j at intersection i at time-step k_i

Notation	Description
$G_i(k_i)$ (unit of time)	Green time at intersection i at time-step k_i
$G_i^{\min}(\mathcal{P}_i, k_i)$ (unit of time)	Minimum saturated green time greater than zero for each possible phase at intersection i at time-step k_i
$\mathcal{M}_{\mathcal{P}_i}$	Set of movements in phase $\mathcal{P}_i$ that receive the right-of-way
$F_{ji}(\mathcal{P}_i, k_i)$ (veh)	Vehicle discharge of movement j in phase $\mathcal{P}_i$ at intersection i at time-step k_i
$v_i(\mathcal{P}_i, k_i)$ (veh/unit of time)	Effective outflow rate at intersection i at time-step k_i given phase $\mathcal{P}_i$
$F_{ji}^{\max}(\mathcal{P}_i, k_i)$ (veh)	Maximum vehicle discharge of movement j at intersection i at time-step k_i given phase $\mathcal{P}_i$
$\mathcal{P}^*_{i,\text{Iter1}}(k_i)$	Selected phase in the first iteration at time-step k_i at intersection i
$\mathcal{P}_i^{\text{Iter2}}(k_i)$	Set of possible phases obtained in the second iteration at time-step k_i at intersection i
$\mathcal{P}^*_{i,\text{Set-Iter2}}(k_i)$	Set of selected phases in the second iteration at time-step k_i at intersection i
α, K, ξ, ϵ	Constants
n_i	Number of time-steps of the control algorithm applied to intersection i during the control time period $[0, T]$
$\mathcal{J}_{\text{E}}$	Set of entrance links to the network
$q_l^{\text{E}}(t)$ (veh/unit of time)	The inflow demand to the network at time t from entrance link $l \in \mathcal{J}_{\text{E}}$
$\mathcal{J}_{\text{in}}$	Set of internal network links
$X(t)$	Queuing process
$Q_{ji}(t)$ (veh)	Queue size of movement j at intersection i at time $t \geq 0$
$Q(t) = [Q_{ji}](t)$	Vector of queue sizes in the network
$q_{ji}^{\text{out}}(t)$ (veh/unit of time)	Effective outflow of movement j at intersection i
$V(Q(t))$	Storage function,
θ (unit of time)	Detection interval
u^{a} (unit of distance/unit of time)	Link free flow speed
D (unit of distance)	Distance that can be traveled in each link during each detection interval
η	Number of matrices (or sections) in the arrival flow estimation process
$q_j^{\text{arr-set}}(K)$	Set of matrices required in the arrival flow estimation process to store the data in different detection time instances for movement j

Appendix B. Arrival flow estimation

For arrival flow estimation, we use a discretization approach in which we consider two effective factors: (i) the queue length in each lane at phase transition point and (ii) the time that it takes the platoon of vehicles to reach the end of the queue. Here, in Appendix B, the intersection notation i has been dropped for brevity. First, we consider a detection interval, θ (s). Based on the detection interval and free flow speed u^{a} (m/s) of the link, the maximum distance, D (m), that can be traveled in each link during each detection interval is $D = \theta u^{\text{a}}$. Accordingly, we divide the link length to η sections, where $\eta = \frac{\Delta}{D}$. For each section, a matrix is considered. When the count of vehicles are read at the upstream of the link at the end of each detection interval, the count data is converted to flow data and is stored in the matrix $q_{j,\eta}^{\text{arr}}(k_i)$. At the end of the next detection interval, this data is moved to the matrix in the adjacent downstream section, $q_{j,\eta-1}^{\text{arr}}(k_i)$, and the new read data is stored in the matrix $q_{j,\eta}^{\text{arr}}(k_i)$. This process continues to build $q_j^{\text{arr-set}}(k_i) = \left\{ q_{j,1}^{\text{arr}}(k_i), q_{j,2}^{\text{arr}}(k_i), \ldots, q_{j,\eta}^{\text{arr}}(k_i) \right\}$, including η matrices as below:

$$q_j^{\text{arr-set}}(k_i) = \begin{cases} q_{j,1}^{\text{arr}}(k_i) := q_{j,2}^{\text{arr}}(k_i - 1), \\ q_{j,2}^{\text{arr}}(k_i) := q_{j,3}^{\text{arr}}(k_i - 1), \\ . \\ . \\ . \\ q_{j,\eta-1}^{\text{arr}}(k_i) := q_{j,\eta}^{\text{arr}}(k_i - 1), \\ q_{j,\eta}^{\text{arr}}(k_i) := q_{j,\text{input}}^{\text{arr}}(k_i), \end{cases} \tag{B.1}$$

where $q_j^{\text{arr-set}}(k_i)$ is the set of arrival flow matrices at the time step k_i for each lane; and $q_{j,1}^{\text{arr}}(k_i)$, $q_{j,\eta}^{\text{arr}}(k_i)$, $q_{j,\text{input}}^{\text{arr}}(k_i)$, respectively, are the matrices for storing the data of the most upstream section, the data of the most downstream section, and the data which is read at the end of each detection interval at the upstream of the link.

Depending on the position of the last queued vehicle at the end of the detection interval, i.e. the estimated queue length $x_j^0(k_i)$, the related matrix, $q_j^{\text{arr}}(k_i) \subseteq q_j^{\text{arr-set}}(k_i)$, based on the following conditions is selected to determine the arrival flow, which ensures

Table C.4
Comparison of the proposed method and green wave method in the arterial case.

	Speed (km/h)			Travel time (s/km)			Total queue (veh)			Max queue (veh)		
	Minor	Major	Combined	Minor	Major	Combined	Minor	Major	Combined	Minor	Major	Combined
Green wave method	25.9	42.3	34.1	87.8	39.3	63.5	51.9	8.9	30.4	26.3	7.4	16.9
Proposed method	35.4	36.9	36.2	46.6	47.2	46.9	14.1	14.6	14.3	12.8	12.2	12.5

to a high degree that the approaching platoon of vehicles will reach the end of the queue.

$$q_{ji}^{\mathrm{arr}}(k_i) = \begin{cases} q_{j,1}^{\mathrm{arr}}(k_i) & \text{if} \quad 0 \le x_j^0(k_i) < D_{j,1}(k_i) \\ q_{j,2}^{\mathrm{arr}}(k_i) & \text{if} \quad D_{j,1}(k_i) \le x_j^0(k_i) < D_{j,2}(k_i) \\ . & \\ . & \\ . & \\ q_{j,\eta-1}^{\mathrm{arr}}(k_i) & \text{if} \quad D_{j,\eta-2}(k_i) \le x_j^0(k_i) < D_{j,\eta-1}(k_i) \\ q_{j,\eta}^{\mathrm{arr}}(k_i) & \text{if} \quad D_{j,\eta-1}(k_i) \le x_j^0(k_i) < D_{j,\eta}(k_i). \end{cases} \tag{B.2}$$

Appendix C. Evaluation of the performance of the method compared to a coordinated method

We designed a 10-intersection arterial for this experiment. In this setup, we considered a one-directional three-lane W-E arterial road (as the major road) including two through lanes and one left turn lane, that is crossed by 10 one-directional two-lane S-N collector approaches (as minor roads) each with one through and one right turn lanes.

We used a green wave method with a 25-s offset between traffic signals and a 68-s fixed cycle time for all signals for the evaluation purpose. We ran 10 replications in AIMSUN and collected the data of four evaluation performance measures including speed (km/h), travel time (s/km), total queue (veh), and maximum queue (veh), averaged separately for minor, major, and combined minor and major sections. The results are averaged over the 10 replications. As listed in Table C.4, the results show that our method outperforms the coordinated green wave control method in the arterial although the performance of the green wave method in major sections of the arterial surpasses our proposed method.

The above results demonstrate that controlling a network with multiple overlapping (two-directional) arterials requires complex coordination schemes such that widely-used green waves might be subpar. Note that the demand in the replications follows similar demand patterns in the paper during a 3-hour simulation period, starting from 1100 veh/15 min (8:00 am to 8:15 am), increasing up to a maximum of 2750 veh/15 min (9:15 am to 9:45 am), and then decreasing back to 1100 veh/15 min (10:45 am to 11:00 am).

References

Aboudolas, K.M.A.E., Papageorgiou, M., Kouvelas, A., Kosmatopoulos, E., 2010. A rolling-horizon quadratic-programming approach to the signal control problem in large-scale congested urban road networks. Transp. Res. C 18 (5), 680–694.

Akçelik, Rahmi, 1999. A Queue Model for HCM 2000. ARRB Transportation Research Ltd., Vermont South, Australia.

Allsop, Richard E., 1971. Delay-minimizing settings for fixed-time traffic signals at a single road junction. IMA J. Appl. Math. 8 (2), 164–185.

Balaji, P.G., German, X., Srinivasan, Dipti, 2010. Urban traffic signal control using reinforcement learning agents. IET Intell. Transp. Syst. 4 (3), 177–188.

Ban, Xuegang Jeff, Hao, Peng, Sun, Zhanbo, 2011. Real time queue length estimation for signalized intersections using travel times from mobile sensors. Transp. Res. C 19 (6), 1133–1156.

Burguillo-Rial, Juan C., Rodríguez-Hernández, Pedro S., Montenegro, Enrique Costa, Castiñeira, Felipe Gil, 2012. History-based self-organizing traffic lights. Comput. Inform. 28 (2), 157–168.

Byrnes, C.I., Isidori, A., Willems, J.C., 1991. Passivity, feedback equivalence, and the global stabilization of minimum phase nonlinear systems. IEEE Trans. Automat. Control 36 (11), 1228–1240.

Chow, Andy H.F., Sha, Rui, Li, Shuai, 2019. Centralised and decentralised signal timing optimisation approaches for network traffic control. Transp. Res. C.

Chow, Andy H.F., Sha, Rui, Li, Ying, 2020. Adaptive control strategies for urban network traffic via a decentralized approach with user-optimal routing. IEEE Trans. Intell. Transp. Syst. 21 (4), 1697–1704. http://dx.doi.org/10.1109/TITS.2019.2955425.

Christofa, Eleni, Papamichail, Ioannis, Skabardonis, Alexander, 2013. Person-based traffic responsive signal control optimization. IEEE Trans. Intell. Transp. Syst. 14 (3), 1278–1289.

Daganzo, Carlos F., 1995. The cell transmission model, part II: network traffic. Transp. Res. B 29 (2), 79–93.

Diakaki, Christina, Dinopoulou, Vaya, Aboudolas, Kostas, Papageorgiou, Markos, Ben-Shabat, Elia, Seider, Eran, Leibov, Amit, 2003. Extensions and new applications of the traffic-responsive urban control strategy: Coordinated signal control for urban networks. Transp. Res. Rec. 1856 (1), 202–211.

Dinopoulou, Vaya, Diakaki, Christina, Papageorgiou, Markos, 2006. Applications of the urban traffic control strategy TUC. European J. Oper. Res. 175 (3), 1652–1665.

Emami, Azadeh, Sarvi, Majid, Bagloee, Saeed Asadi, 2021. Network-wide traffic state estimation and rolling horizon-based signal control optimization in a connected vehicle environment. IEEE Trans. Intell. Transp. Syst..

Erera, Alan L., Lawson, Tim W., Daganzo, Carlos F., 1998. Simple, generalized method for analysis of traffic queue upstream of a bottleneck. Transp. Res. Rec. 1646 (1), 132–140.

Feng, Yiheng, Head, K. Larry, Khoshmagham, Shayan, Zamanipour, Mehdi, 2015. A real-time adaptive signal control in a connected vehicle environment. Transp. Res. C 55, 460–473.

Geroliminis, Nikolas, Haddad, Jack, Ramezani, Mohsen, 2012. Optimal perimeter control for two urban regions with macroscopic fundamental diagrams: A model predictive approach. IEEE Trans. Intell. Transp. Syst. 14 (1), 348–359.
Geroliminis, Nikolas, Skabardonis, Alexander, 2011. Identification and analysis of queue spillovers in city street networks. IEEE Trans. Intell. Transp. Syst. 12 (4), 1107–1115.
Gershenson, Carlos, 2007. Design and Control of Self-Organizing Systems. CopIt Arxives.
Gregoire, Jean, Qian, Xiangjun, Frazzoli, Emilio, De La Fortelle, Arnaud, Wongpiromsarn, Tichakorn, 2014. Capacity-aware backpressure traffic signal control. IEEE Trans. Control Netw. Syst. 2 (2), 164–173.
Haddad, Jack, De Schutter, Bart, Mahalel, David, Ioslovich, Ilya, Gutman, Per-Olof, 2010. Optimal steady-state control for isolated traffic intersections. IEEE Trans. Automat. Control 55 (11), 2612–2617.
Kouvelas, Anastasios, Lioris, Jennie, Fayazi, S. Alireza, Varaiya, Pravin, 2014. Maximum pressure controller for stabilizing queues in signalized arterial networks. Transp. Res. Rec. 2421 (1), 133–141.
Lämmer, Stefan, Helbing, Dirk, 2008. Self-control of traffic lights and vehicle flows in urban road networks. J. Stat. Mech. Theory Exp. 2008 (04), P04019.
Le, Tung, Kovács, Péter, Walton, Neil, Vu, Hai L., Andrew, Lachlan L.H., Hoogendoorn, Serge S.P., 2015. Decentralized signal control for urban road networks. Transp. Res. C 58, 431–450.
Lee, Seunghyeon, Wong, S.C., Varaiya, Pravin, 2017. Group-based hierarchical adaptive traffic-signal control part I: Formulation. Transp. Res. B 105, 1–18.
Lee, Seunghyeon, Xie, Kun, Ngoduy, Dong, Keyvan-Ekbatani, Mehdi, 2019. An advanced deep learning approach to real-time estimation of lane-based queue lengths at a signalized junction. Transp. Res. C 109, 117–136.
Li, Li, Jabari, Saif Eddin, 2019. Position weighted backpressure intersection control for urban networks. Transp. Res. B 128, 435–461.
Li, Ye, Mohajerpoor, Reza, Ramezani, Mohsen, 2021. Perimeter control with real-time location-varying cordon. Transp. Res. B 150, 101–120.
Lighthill, Michael James, Whitham, G.B., 1955. On kinematic waves I. Flood movement in long rivers. Proc. R. Soc. Lond. Ser. A Math. Phys. Sci. 229 (1178), 281–316.
Little, John D.C., Kelson, Mark D., Gartner, Nathan H., 1981. MAXBAND: A Versatile Program for Setting Signals on Arteries and Triangular Networks. Alfred P. Sloan School of Management, Massachusetts Institute of Technology.
Lo, Hong K., Chow, Andy H.F., 2004. Control strategies for oversaturated traffic. J. Transp. Eng. 130 (4), 466–478.
Mehrabipour, Mehrzad, Hajbabaie, Ali, 2017. A cell-based distributed-coordinated approach for network level signal timing optimization. Comput.-Aided Civ. Infrastruct. Eng. 32 (7), 599–616.
Michalopoulos, Panos G., Stephanopoulos, George, 1977. Oversaturated signal systems with queue length constraints-II: Systems of intersections. Transp. Res. 11 (6), 423–428.
Michalopoulos, Panos G., Stephanopoulos, Gregory, Stephanopoulos, George, 1981. An application of shock wave theory to traffic signal control. Transp. Res. B 15 (1), 35–51.
Mohajerpoor, Reza, Ramezani, Mohsen, 2019. Mixed flow of autonomous and human-driven vehicles: Analytical headway modeling and optimal lane management. Transp. Res. C 109, 194–210.
Mohajerpoor, Reza, Saberi, Meead, Ramezani, Mohsen, 2019. Analytical derivation of the optimal traffic signal timing: Minimizing delay variability and spillback probability for undersaturated intersections. Transp. Res. B 119, 45–68.
Mohebifard, Rasool, Hajbabaie, Ali, 2019. Optimal network-level traffic signal control: A benders decomposition-based solution algorithm. Transp. Res. B 121, 252–274.
Nie, Xiaojian, Zhang, H. Michael, 2005. A comparative study of some macroscopic link models used in dynamic traffic assignment. Netw. Spat. Econ. 5 (1), 89–115.
Osorio, Carolina, Bierlaire, Michel, 2009. An analytic finite capacity queueing network model capturing the propagation of congestion and blocking. European J. Oper. Res. 196 (3), 996–1007.
Osorio, Carolina, Selvam, Krishna Kumar, 2017. Simulation-based optimization: achieving computational efficiency through the use of multiple simulators. Transp. Sci. 51 (2), 395–411.
Ramezani, Mohsen, Geroliminis, Nikolas, 2015. Queue profile estimation in congested urban networks with probe data. Comput.-Aided Civ. Infrastruct. Eng. 30 (6), 414–432.
Ramezani, Mohsen, de Lamberterie, Nicolas, Skabardonis, Alexander, Geroliminis, Nikolas, 2017. A link partitioning approach for real-time control of queue spillbacks on congested arterials. Transportmetr. B 5 (2), 177–190.
Richards, Paul I., 1956. Shock waves on the highway. Oper. Res. 4 (1), 42–51.
Rinaldi, Marco, Tampère, Chris M.J., 2015. An extended coordinate descent method for distributed anticipatory network traffic control. Transp. Res. B 80, 107–131.
Robertson, Dennis I., 1969. TRANSYT: a traffic network study tool.
Safadi, Yazan, Haddad, Jack, 2021. Optimal combined traffic routing and signal control in simple road networks: an analytical solution. Transportmetr. A 17 (3), 308–339.
Sirmatel, Isik Ilber, Geroliminis, Nikolas, 2021. Stabilization of city-scale road traffic networks via macroscopic fundamental diagram-based model predictive perimeter control. Control Eng. Pract. 109, 104750.
Skabardonis, Alexander, Geroliminis, Nikolas, 2008. Real-time monitoring and control on signalized arterials. J. Intell. Transp. Syst. 12 (2), 64–74.
Smith, M.J., 1980. A local traffic control policy which automatically maximises the overall travel capacity of an urban road network. Traffic Eng. Control 21 (HS-030 129).
Smith, Mike, 2011. Dynamics of route choice and signal control in capacitated networks. J. Choice Model. 4 (3), 30–51.
Smith, Mike, 2015. Traffic signal control and route choice: A new assignment and control model which designs signal timings. Transp. Res. C 58, 451–473.
Smith, Michael J., Iryo, Takamasa, Mounce, Richard, Rinaldi, Marco, Viti, Francesco, 2019. Traffic control which maximises network throughput: Some simple examples. Transp. Res. C 107, 211–228.
Srinivasan, Dipti, Choy, Min Chee, Cheu, Ruey Long, 2006. Neural networks for real-time traffic signal control. IEEE Trans. Intell. Transp. Syst. 7 (3), 261–272.
Stevanovic, Aleksandar, Stevanovic, Jelka, So, Jaehyun, Ostojic, Marija, 2015. Multi-criteria optimization of traffic signals: Mobility, safety, and environment. Transp. Res. C 55, 46–68.
Tassiulas, Leandros, Ephremides, Anthony, 1990. Stability properties of constrained queueing systems and scheduling policies for maximum throughput in multihop radio networks. In: 29th IEEE Conference on Decision and Control. IEEE, pp. 2130–2132.
Varaiya, Pravin, 2013. Max pressure control of a network of signalized intersections. Transp. Res. C 36, 177–195.
Vigos, Georgios, Papageorgiou, Markos, Wang, Yibing, 2008. Real-time estimation of vehicle-count within signalized links. Transp. Res. C 16 (1), 18–35.
Viti, Francesco, Van Zuylen, Henk J., 2010. Probabilistic models for queues at fixed control signals. Transp. Res. B 44 (1), 120–135.
Webster, Fo Vo, 1958. Traffic Signal Settings. Tech. rep..
Wongpiromsarn, Tichakorn, Uthaicharoenpong, Tawit, Wang, Yu, Frazzoli, Emilio, Wang, Danwei, 2012. Distributed traffic signal control for maximum network throughput. In: 2012 15th International IEEE Conference on Intelligent Transportation Systems. IEEE, pp. 588–595.
Wu, Xinkai, Liu, Henry X., 2011. A shockwave profile model for traffic flow on congested urban arterials. Transp. Res. B 45 (10), 1768–1786.
Xie, Xiao-Feng, Smith, Stephen F., Lu, Liang, Barlow, Gregory J., 2012. Schedule-driven intersection control. Transp. Res. C 24, 168–189.

Xu, Biao, Ban, Xuegang Jeff, Bian, Yougang, Li, Wan, Wang, Jianqiang, Li, Shengbo Eben, Li, Keqiang, 2018. Cooperative method of traffic signal optimization and speed control of connected vehicles at isolated intersections. IEEE Trans. Intell. Transp. Syst. 20 (4), 1390–1403.

Yang, Kaidi, Guler, S. Ilgin, Menendez, Monica, 2016. Isolated intersection control for various levels of vehicle technology: Conventional, connected, and automated vehicles. Transp. Res. C 72, 109–129.

Yperman, Isaak, Logghe, Steven, Immers, Ben, 2005. The link transmission model: An efficient implementation of the kinematic wave theory in traffic networks. In: Proceedings of the 10th EWGT Meeting. Poznan Poland. pp. 122–127.

Zhang, Guohui, Wang, Yinhai, 2010. Optimizing minimum and maximum green time settings for traffic actuated control at isolated intersections. IEEE Trans. Intell. Transp. Syst. 12 (1), 164–173.

Zhang, Chao, Xie, Yuanchang, Gartner, Nathan H., Stamatiadis, Chronis, Arsava, Tugba, 2015. AM-band: an asymmetrical multi-band model for arterial traffic signal coordination. Transp. Res. C 58, 515–531.